An Improved Butterfly Optimization Algorithm for Numerical Optimization and Parameter Identification of Photovoltaic Model

Xueyan Ru*

Abstract—**Photovoltaic (PV) model parameter identification is a nonlinear, multivariate and strong coupling optimization problem, which is of crucial importance for PV systems. In view of the shortcomings of traditional identification methods, such as low accuracy and slow convergence speed, this paper proposes an improved butterfly optimization algorithm (BOA) based on chaotic learning and terminal elimination strategy, called CTBOA. Firstly, a novel fragrance factor is designed to enhance the leading role of the optimal butterfly and accelerate the convergence speed. Secondly, a chaotic learning strategy is utilized, which adopts an improved chaotic map to guide the butterflies to learn towards the best individual, thereby enhancing the convergence accuracy. Finally, the terminal elimination strategy is used to initialize the positions of the 5 poorest individuals to increase population diversity. In addition, CTBOA is evaluated with 3 BOA variants and 6 well-known algorithms with CEC2022 test set. Then CTBOA is applied to the parameters identification of 4 PV models, and demonstrates remarkable competitiveness in terms of convergence performance and identification accuracy compared with 9 comparison algorithms. The comprehensive analysis shows that CTBOA is able to identify the best parameters superior to comparison methods, proving its capability in numerical optimization and PV model parameters identification.**

Index Terms—**Photovoltaic model, parameter identification, chaotic learning strategy, numerical optimization**

I. Introduction

In the past few decades, renewable energy has received a lot of attention as an alternative to fossil energy. PV power generation takes an essential position in today's renewable energy, and its penetration rate in the grid is very high. The PV cell model is an important part of the PV system. The study of PV systems requires accurate modeling of PV cells [1]. Generally, the fundamental models of equivalent circuits for PV cells are single diode model (SDM), double diode model (DDM) and triple diode model (TDM), the SDM is simple and has a fast dynamic response with 5 parameters to be identified [2]. The DDM considers the compound influence in the neutral areas of the junction and therefore models the PV cell more accurately with its 7 parameters to be identified [3]. TDM has a complete PV cell loss characterization with 9 parameters to be identified [4]. The equivalent circuits of the above 3 models are implicitly nonlinear equations and the unknown parameters are difficult to identify precisely due to variations in temperature and irradiation intensity. The parameters of PV model directly affect the dynamic performance of the system, therefore, devising an accurate and reliable parameter identification method is of great significance.

Different methods have been applied to identify the unknown parameters of the PV model, like numerical method, meta-heuristic algorithm, etc. The main disadvantage of Newton-Raphson and other numerical techniques is that they require a lot of calculation to converge, but improper selection of initial values will not get accurate results [5]. The main advantage of meta-heuristic algorithms lies in the fact it does not require continuity and microscopicity of the objective function and show effectiveness in solving engineering problems, like particle swarm optimization algorithm (PSO) [6], improved grey wolf optimizer (I-GWO) [7], triple shake algorithm (TSA) [8], enhanced sparrow search algorithm (ESSA) [9], improved whale optimization algorithm (EIWOA) [10], enhanced particle swarm optimization algorithm (SCOPSO) [11], adaptive filtering algorithm (AFA) [12], differential evolution algorithm with dynamic control factors [13].

To solve the problem of PV cell parameters identification, PSO has been proposed in [6], which overcomes the problem of encountering locally optimal solutions and can efficiently obtain accurate fitted parameters to complete the simulation of I-V characteristics. Subudhi et al. [14] introduced a algorithm to identify the parameters of PV modules using bacterial foraging optimization algorithm (BFO) for PV modules under different test conditions, the model parameters obtained by this method are more accurate as compared to Newton-Raphson method, PSO and enhanced simulated annealing (SA), but this method was only applied to identify the unknown parameters of PV modules with SDM. In [15], a genetic algorithm (GA) has been utilized for this problem. In [16], a multiple learning backtracking search algorithm (BSA) was utilized to recognize the parameters of PV models, the results of the experiment showed that the proposed BSA was able to identify the parameters of the SDM and DDM PV cells, however, computational efficiency may be reduced when determining the parameters of larger systems. In [17], an improved differential evolution algorithm (DE) was used to identify PV parameters and improve convergence performance by introducing a cross-rate ranking mechanism, however, using the differential evolution algorithm requires a longer iterative process to reach the PV model parameters. For the same problem, Huiling Chen et al. [18] introuduced a diversity-enhanced Harris hawk optimization (HHO) algorithm, and the experimental results proved the excellent properties of the proposed method in identifying the key parameters of the PV model, but the computation time is long due to the introduction of two operators. In [19], a

Manuscript received March 26, 2024; revised December 26, 2024.

Xueyan Ru is a lecturer of School of Electronic and Electrical Engineering, Bengbu University, Bengbu, Anhui 233000, China. (Corresponding author to provide phone: 8618656257687; e-mail: ruxy@bbc.edu.cn)

whale optimization algorithm (WOA) was developed for the calculation of unknown parameters of PV models. A seagull optimization algorithm (SOA) was suggested in [20] for the same problem. In [21], Xiaobing Yu et al. proposed an improved grey wolf optimizer (GWO) to update the positions of individuals using different search strategies for superior and inferior populations, the results show that the method increases the population diversity and solves the parameter identification problem for 5 PV models.

Although many methods have been developed to solve this problem, since PV model parameters identification is a complex problem, a considerable number of methods have difficulty in obtaining a globally optimal solution. Therefore, finding a competitive algorithm that can accurately and reliably identify the parameters of different PV models remains a challenging task.

Butterfly optimization algorithm (BOA) is a new population based heuristic proposed by Arora Sankalap et al. [22]. Due to its flexibility and efficiency, BOA and its variants have been applied to a wide range of real-world optimization problems such as numerical optimization problems [23], engineering problems [24].

As a young algorithm, BOA suffers from slow convergence speed, low convergence accuracy and poor population diversity. Moreover, to the best of my limited knowledge, there are few literature reports on the use of BOA and its variants for PV model parameter identification problems. To this end, this paper proposes a butterfly optimization algorithm based on the improved fragrance factor, chaotic learning and final elimination for identifying PV model parameters. Firstly, the fragrance factor of BOA is improved to enhance the leading role of the optimal butterfly individual and accelerate the convergence speed. Secondly, a chaotic learning strategy (CLS) is proposed, which employs improved chaotic map to guide the butterflies to learn towards the best individual, to improve the precision of convergence. Finally, the positions of the poorest 5 individuals are initially initialized using a final elimination strategy to increase population diversity.

The main contributions of this paper are as follows.

(1) An improved BOA based on chaotic learning and final elimination is proposed for identifying PV model parameters.

(2) A novel fragrance factor is designed for BOA to accelerate the convergence speed.

(3) A chaotic learning strategy is introduced for increasing the search capability to avoid falling into local optima, while a final elimination strategy is utilized to enhance the population diversity.

(4) The performance of the proposed CTBOA is tested against the comparison algorithms with CEC2022 test set.

(5) CTBOA is applied to four PV parameter identification problems.

The rest of the paper is organized as follows.

- Section II gives the PV model problem description.
- Section III describes BOA and the proposed CTBOA.
- Section IV provides the performance of CTBOA in CEC2022 test set.
- Section V identifies the parameters of 4 PV models.
- Section VI discusses the conclusions and future work.

II. Problem Description

Common PV models include SDM, DDM and TDM [13], the PV module model consists of a number of PV cells connected in series and/or in parallel, and their equivalent circuits is shown in Figure 1. Switches S_1 and S_2 are turned off, this is SDM. And, S_1 and S_2 are successively turned on, DDM and TDM are successively formed. In addition, the root mean square error (RMSE) is used as objective function.

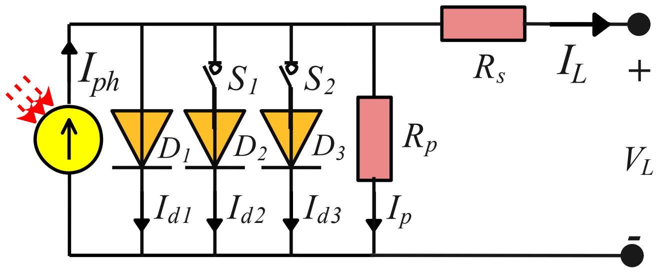

Fig. 1: PV cell model.

A. SDM of PV cell

The equivalent circuit diagram of the SDM consists of a current source I_{ph}, a diode D_1, a parallel resistor R_{p} and a series resistor R_s. The output current I_L of the SDM is shown in Eq.(1).

$$I_L = I_{\text{ph}} - I_{d1} - I_p \tag{1}$$

Where I_{ph} represent the photo-generated current of the PV cell, I_{d1} represent the electric current that flows through D_1, I_p represents the current on R_p, and I_{d1} is calculated as Eq.(2).

$$I_{\text{d1}} = I_{\text{sd1}} \cdot [e^{\frac{q\cdot(V_L+R_s\cdot I_L)}{n_1\cdot k_B\cdot T_K}} - 1] \tag{2}$$

Where I_{sd1} and n_1 are the reverse saturation current and ideal factor of D_1, respectively. q is the electron charge $(1.602176 \cdot 10^{-19}C)$, k_B is a constant $(1.380650 \cdot 10^{-23}J/K)$, and T_K denotes the temperature of the cell.

In summary, Eq.(1) is expressed as Eq.(3).

$$I_L = I_{\text{ph}} - I_{\text{sd1}} \cdot [e^{\frac{q\cdot(V_L+R_s\cdot I_L)}{n_1\cdot k_B\cdot T_K}} - 1] - \frac{V_L + R_s \cdot I_L}{R_p} \tag{3}$$

According to Eq.(3), the SDM has 5 parameters to be identified, which are I_{ph}, I_{sd1}, R_p, R_s and n_1.

B. DDM of PV cell

Compared with SDM, DDM considers the influence of the combined current loss in the depletion region [25]. The DDM has an extra diode in parallel wired to the current source than the SDM, and I_L is calculated through Eq.(4).

$$\begin{aligned} I_L =& I_{ph} - I_{sd1} \cdot \left[e^{\left(\frac{q\cdot(V_L+R_s\cdot I_L)}{n_1\cdot k_B\cdot T_K}\right)} - 1 \right] \\ & - I_{sd2} \cdot \left[e^{\frac{q\cdot(V_L+R_s\cdot I_L)}{n_2\cdot k_B\cdot T_K}} - 1 \right] - \frac{V_L + R_s \cdot I_L}{R_p} \end{aligned} \tag{4}$$

Where I_{sd1}, I_{sd2}, n_1 and n_2 are the saturation currents and ideal factors of diodes D_1 and D_2, respectively. According to Eq.(4), the PV model built with DDM has 7 parameters to be identified, which are I_{ph}, I_{sd1}, I_{sd2}, R_p, R_s , n_1 and n_2.

C. TDM of PV cell

TDM can more comprehensively characterize the loss of PV cells, I_L for TDM is given in Eq.(5).

$$\begin{aligned} I_L =& I_{ph} - I_{sd1} \cdot \left[e^{\frac{q \cdot (V_L + R_s \cdot I_L)}{n_1 \cdot k_B \cdot T_K}} - 1 \right] \\ &- I_{sd2} \cdot \left[e^{\frac{q \cdot (V_L + R_s \cdot I_L)}{n_2 \cdot k_B \cdot T_K}} - 1 \right] - \frac{V_L + R_s \cdot I_L}{R_p} \\ &- I_{sd3} \cdot \left[e^{(\frac{q \cdot (V_L + R_s \cdot I_L)}{n_3 \cdot k_B \cdot T_K})} - 1 \right] \end{aligned} \tag{5}$$

According to Eq.(5), it can be seen that the PV model by TDM has 9 parameters to be identified, which are I_{ph}, I_{sd1}, I_{sd2}, I_{sd3}, R_p, R_s, n_1, n_2 and n_3.

D. PV module model

The equivalent circuit of PV module model is given in Figure 2. Where N_s and N_p stand for the amounts of series and parallel PV models. I_L of the PV module model based on TDM obtained with Eq.(6).

$$\begin{aligned} I_L =& N_p \cdot I_{ph} - \frac{V_L/N_s + R_s \cdot I_L/N_p}{R_p/N_p} \\ &- N_p \cdot I_{sd1} \cdot \left[e^{\frac{q \cdot (V_L/N_s + R_s \cdot I_L/N_p)}{n_1 \cdot k_B \cdot T_K}} - 1 \right] \\ &- N_p \cdot I_{sd2} \cdot \left[e^{\frac{q \cdot (V_L/N_s + R_s \cdot I_L/N_p)}{n_2 \cdot k_B \cdot T_K}} - 1 \right] \\ &- N_p \cdot I_{sd3} \cdot \left[e^{\frac{q \cdot (V_L/N_s + R_s \cdot I_L/N_p)}{n_3 \cdot k_B \cdot T_K}} - 1 \right] \end{aligned} \tag{6}$$

E. Objective function

Parameter identification for PV models usually uses root mean square error to quantify the variance [16], it is defined as Eq.(7).

$$\min f(\overrightarrow{X}) = RMSE(\overrightarrow{X}) = \sqrt{\frac{1}{M} \sum_{i=1}^{M} (I_{L,mea}^i - I_{L,iden}^i(\overrightarrow{X}))^2} \tag{7}$$

Among them, M is the quantity of experimental data. $I_{L,mea}$ and $I_{L,iden}$ denote the measured and identified currents, respectively. $\overrightarrow{X}$ represents the parameter vector to be identified.

III. The Proposed Method

This section gives the fundamentals of BOA. With the aim of overcoming the disadvantages of BOA, like low convergence accuracy and poor population diversity, a chaotic learning strategy is introduced, as well as the use of improved fragrance factor and final elimination strategy.

A. Butterfly optimization algorithm

Butterfly optimization algorithm (BOA) is a new intelligent optimization algorithm. The main idea of BOA comes from the foraging behavior of butterflies [26]. Butterflies attract companions by releasing fragrances, and they move toward areas with higher concentrations of fragrances. Each individual butterfly has a location that represents a possible solution. During the initialization phase, butterfly individuals within the population are randomly distributed according to Eq.(8).

$$\overrightarrow{X}_i = \overrightarrow{LB} + r(1, Dim). * (\overrightarrow{UB} - \overrightarrow{LB}) \tag{8}$$

Among them, $[\overrightarrow{LB}, \overrightarrow{UB}]$ are the lower and upper search limits of the solution space, respectively. Dim is the problem dimension, the variable r represents a random number within the range of [0, 1].

In BOA, the fragrance factor determines the movement direction of individual butterfly to a large extent. Each butterfly modifies its position in accordance with the intensity of its own fragrance and the fragrance present in its vicinity. Regions with higher fragrance intensity represent potentially better solution space. Fragrance factor f_i is calculated by Eq.(9).

$$f_i = c \cdot I^a \tag{9}$$

In which c represents the sensory modality, usually taken as 0.01. I denotes the stimulus intensity, which is reliant on the fitness of the optimization objective. a represents a power exponent, computed by Eq.(10).

$$a = 0.1 + 0.2(t/T) \tag{10}$$

Where t and T represent the current iteration and the maximum iterations respectively. In addition, the BOA consists of two key steps,namely global search and local search. These two phases are regulated by a switch probability p, which is assigned a value of 0.8. When $r < p$, the individual will execute a global search, as shown in Eq.(11).

$$\overrightarrow{X_{i-BOA}^{t+1}} = \overrightarrow{X_i^t} + (r^2 \cdot \overrightarrow{gbest} - \overrightarrow{X_i^t}) \cdot f_i \tag{11}$$

Where $\overrightarrow{X_i^t}$ represents the solution vector of the $i-th$ butterfly at $t-th$ iteration, and $\overrightarrow{gbest}$ represents the optimal solution identified among all the solutions at the current stage.

Conversely, the individual performs a local search, as shown in Eq.(12).

$$\overrightarrow{X_{i-BOA}^{t+1}} = \overrightarrow{X_i^t} + (r^2 \cdot \overrightarrow{X_j^t} - \overrightarrow{X_k^t}) \cdot f_i \tag{12}$$

In which, $\overrightarrow{X_j^t}$ and $\overrightarrow{X_k^t}$ are randomly chosen from the solution space as the $j-th$ and $k-th$ butterflies.

B. The proposed CTBOA

1) Improved fragrance factor: The stimulus intensity within the BOA is determined by the fitness of the optimization objective. Given that the optimal values of different optimization problems can differ significantly, the fragrance factor calculated by Eq.(11) is prone to fluctuation, and there may be a situation where the butterfly fragrance is absent, leading to the BOA ceasing to update the butterfly position. Therefore, it is necessary to improve the fragrance factor of butterflies. Since the normalized data can accelerate the solution, the improved flavor factor based on this idea is designed as Eq.(13).

$$I = 1 - \frac{Fitness(\overrightarrow{X_i^t}) - gbestvalue}{worstvalue - gbestvalue} \tag{13}$$

Where $gbestvalue$ and $worstvalue$ are the fitness values corresponding to the optimal and worst positions of the population butterfly, respectively. According to Eq.(9) and Eq.(13), the improved butterfly fragrance factor will not appear the absence of fragrance, and BOA will update the butterfly position according to the new fragrance factor.

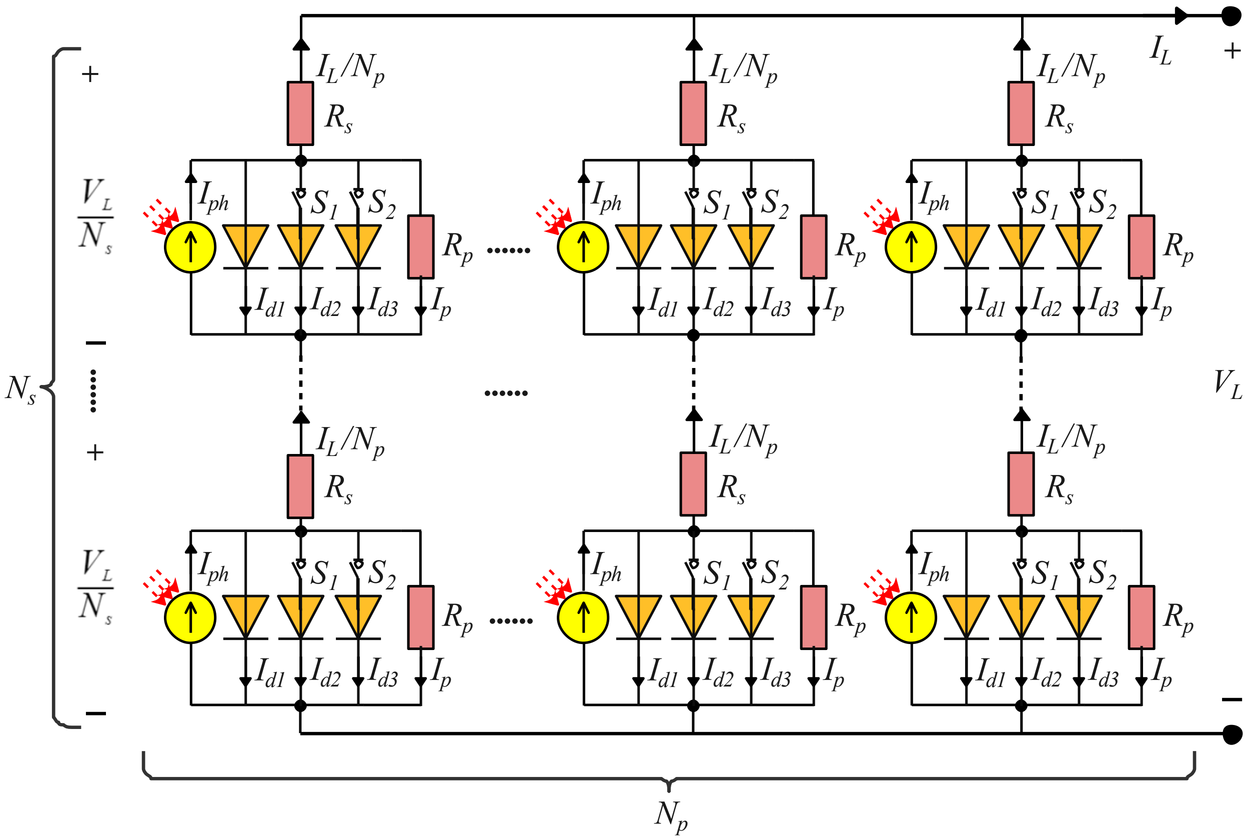

Fig. 2: PV module model.

2) Chaotic Learning Strategy: The chaotic learning strategy comprises a chaotic phase and a learning phase, and the details are as follows.

(a) Chaotic phase. Chaos is commonly found in nonlinear systems [27]. It is capable of enhancing the global searching capacity of the algorithm and improve the solving precision of the problem. Tent chaotic perturbation creates the chaotic variable via Tent chaotic mapping. Then it is introduced into the solution space of the problem to be addressed and ultimately perturbs the individual in a chaotic manner. The Tent chaotic mapping is presented in Eq.(14).

$$z_{i+1} = (2z_i)mod1 + r \cdot \frac{1}{N_T} \tag{14}$$

Where, N_T is the number of chaotic particles. For the purpose of extending the Tent mapping, Eq.(14) is improved and the improved Tent mapping is shown in Eq.(15). The improved Tent chaotic has a wider mapping range ([-1,1]), which is beneficial to enhancing the global search capability of the method.

$$z_{i+1}^{new} = sgn(0.5 - r) \cdot ((2z_i)mod1 + r \cdot \frac{1}{N_T}) \tag{15}$$

Where sgn is the sign function that controls the interference direction.

(b) Learning phase. In a population, $\overrightarrow{gbest}$ is supposed to raise the average value of the population to a certain degree depending on the size of the population, and the formula for mean position is shown in Eq.(16).

$$\overrightarrow{X_m} = (\frac{1}{N}\sum_{i=1}^{N}\overrightarrow{X_{i,1}}, \frac{1}{N}\sum_{i=1}^{N}\overrightarrow{X_{i,2}}, \cdots \frac{1}{N}\sum_{i=1}^{N}\overrightarrow{X_{i,Dim}}) \tag{16}$$

Where, $\overrightarrow{x_{i,j}}$ is the $j-th$ dimension of the $i-th$ butterfly. Define the process of learning the average position towards the $\overrightarrow{gbest}$ of the population as the learning step, as shown in Eq.(17).

$$\overrightarrow{X_{learning}} = z_{i+1}^{new} \cdot r(1, Dim). * (\overrightarrow{gbest} - \overrightarrow{X_m}) \tag{17}$$

The chaotic learning strategy is applied to the butterfly position update with the Eq.(18).

$$\overrightarrow{X_{i-CL}^{t+1}} = \overrightarrow{X_i^t} + \overrightarrow{X_{learning}} \tag{18}$$

The chaotic learning strategy makes the average value learn towards the best individual from various directions, which improves the global and local search ability that helps the method to enhance the accuracy of problem-solving.

3) Final elimination strategy: The final elimination strategy add the diversity of the population by eliminating unfavorable individuals and randomly initializing the locations of the 5 poorest individuals in each iteration based on Eq.(19).

$$\overrightarrow{X_{s[(N-4):N]}} = \overrightarrow{LB} + r(1, Dim). * (\overrightarrow{UB} - \overrightarrow{LB}) \tag{19}$$

Where s is the ordinal number obtained by ordering the fitness from the best to the worst. N is the population size.

C. Framework of CTBOA

The pseudo-code and flowchart can visually demonstrate the framework of CTBOA, as shown in Algorithm 1 and Figure 3, separately.

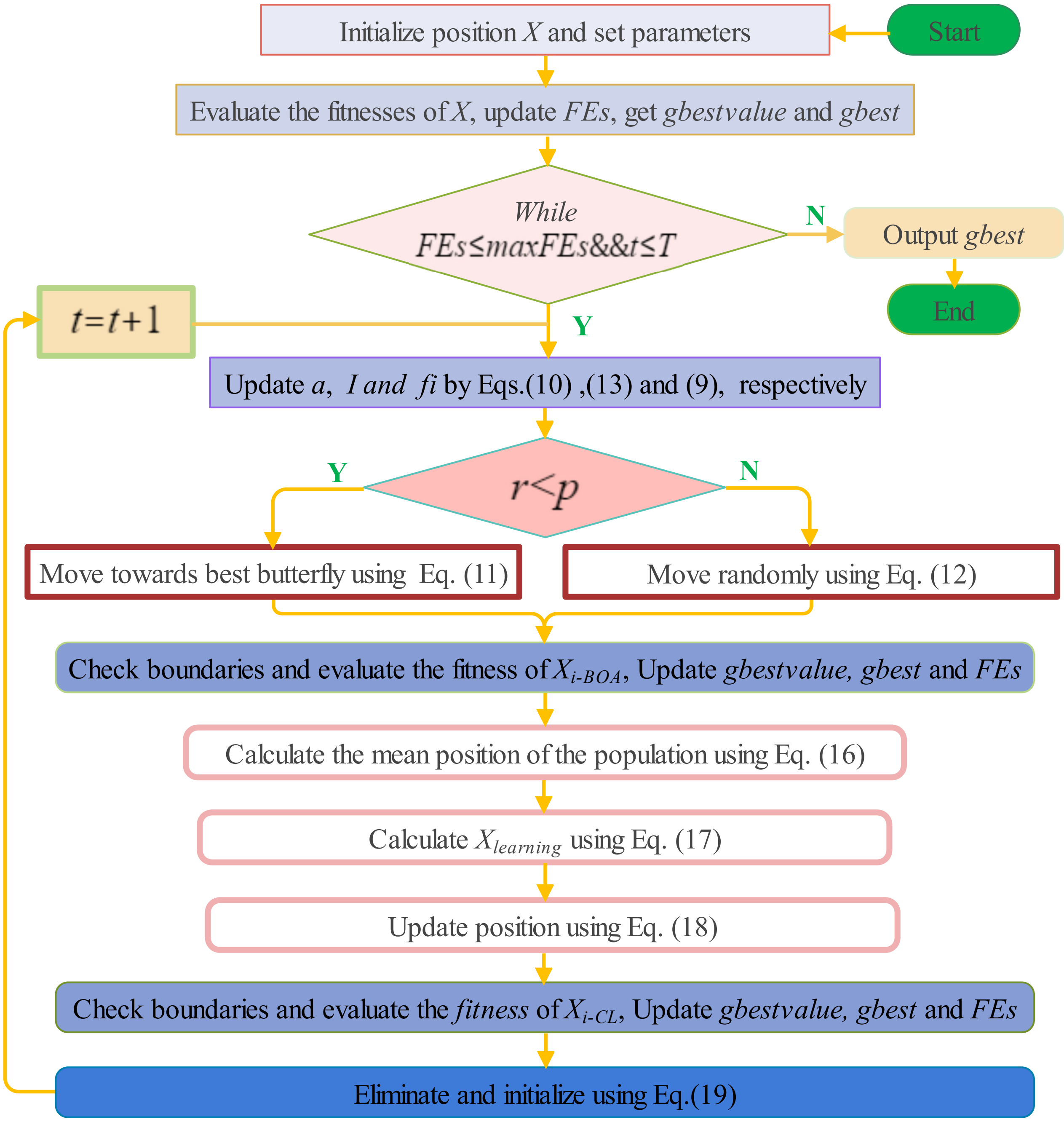

Fig. 3: Flowchart of CTBOA.

IV. Numerical optimization results

A. CEC2022 test functions and parameters setting

In this subsection, the performance of the CTBOA is verified by CEC2022 benchmark test set. For further validation of the properties of CTBOA, 9 competitive comparison algorithms are selected, as listed in Table I. The main information of CEC2022 is shown in Table II. For the impartiality of the experiment, and the evaluation quantity in 10 dimensions (D10) is 200,000. Each function runs independently 30 times. The test platform is Matlab R2021b. The test device is a PC running Microsoft Windows 11 operating system.

B. Search history analysis of CTBOA

In this part, basic function f_2 in CEC2022 is used to verify the performance of CTBOA. In order to present the experimental results in a more straightforward manner, the dimension is set as 2, the population size is set to 4, and the maximum number of iterations is set to 100. The experimental results are illustrated in Figures 4 and 5.

From Figures, the proposed CTBOA has a wider traversal range than BOA on f_2, the convergence speed is faster during the early period, and after multiple searches in the advanced stage, it almost reaches the optimal value of the function, and has a satisfactory ability to escape the local optimal. These improvements result from the proposed chaotic learning strategy, improved fragrance factor and final elimination strategy.

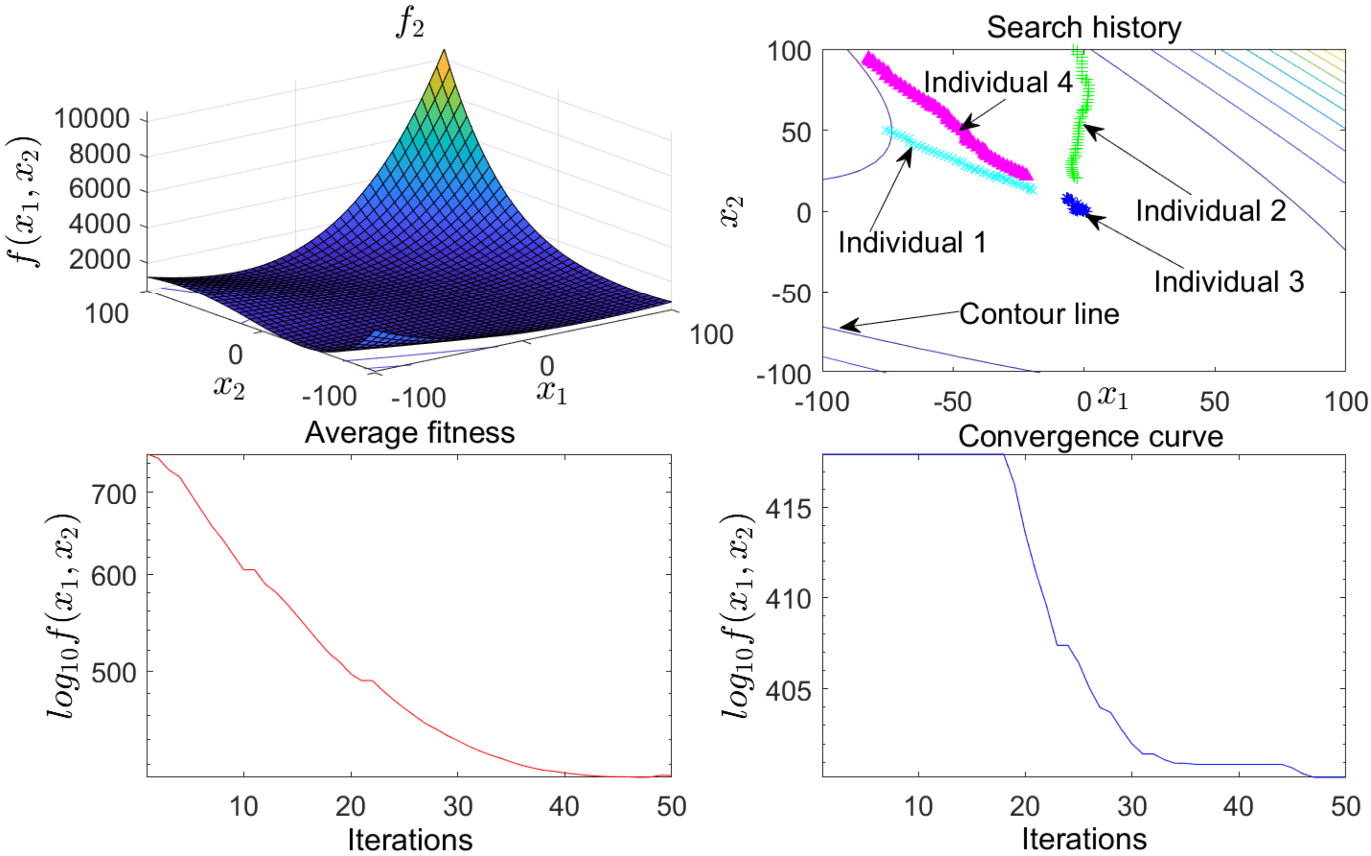

Fig. 4: Search history of original BOA on f_2.

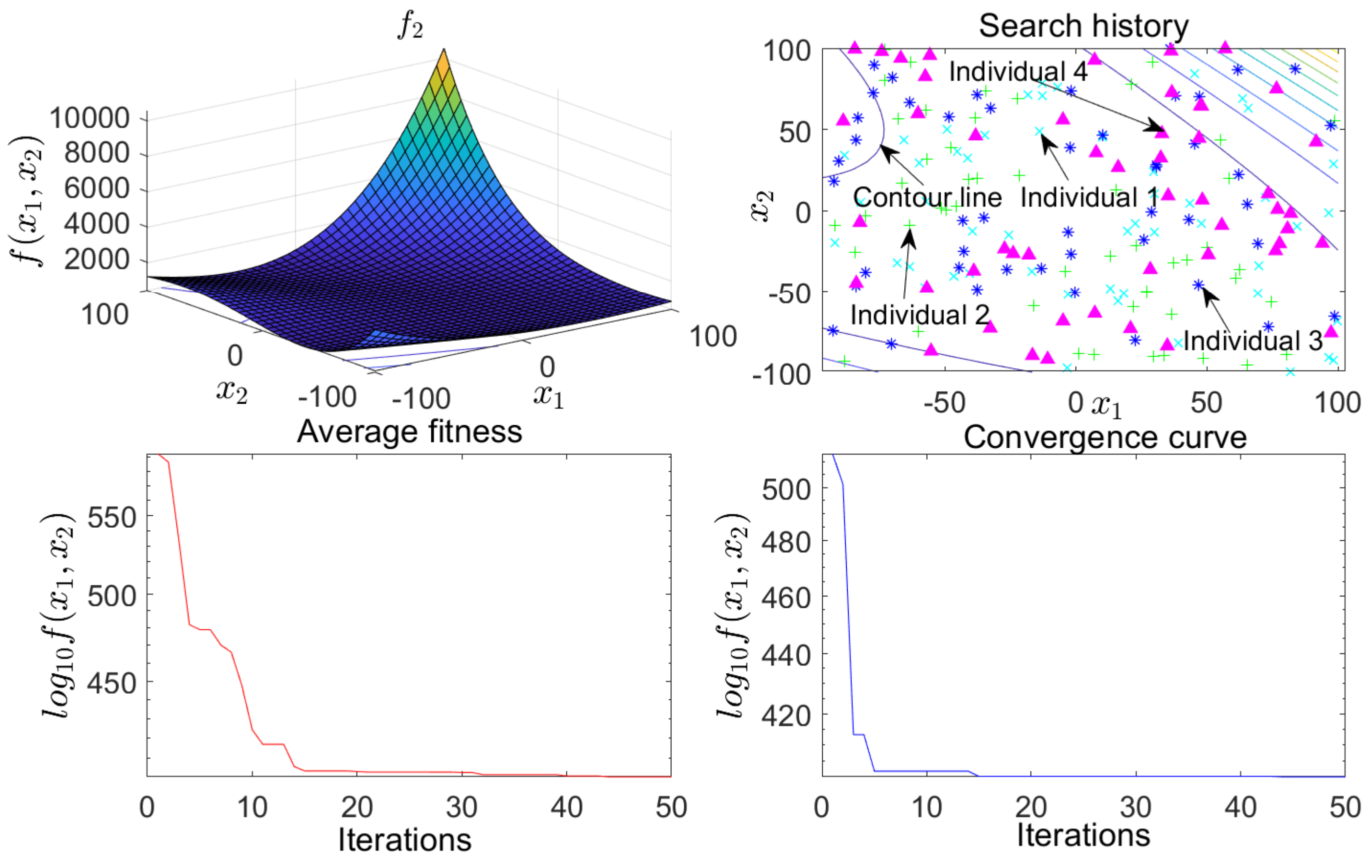

Fig. 5: Search history of CTBOA on f_2.

Algorithm 1: The pseudo-code of CTBOA

Input: Initialize Parameters.
Output: Optimal solution $\overrightarrow{gbest}$.

Randomly initialize population using Eq.(8);
Evaluate the fitnesses of $\overrightarrow{X}$, Update FEs;
Get $gbestvalue$ and $\overrightarrow{gbest}$;
$T = \lceil maxFEs/N \rceil$, $t = 0$;
while $FEs <= maxFEs$ && $t <= T$ **do**
  $t = t + 1$;
  Calculate the power exponent a by Eq.(10);
  for $i = 1$ ***to*** N **do**
    Calculate I and f_i by Eqs.(13) and (9).;
    if $r < p$ **then**
      Move towards best butterfly using Eq.(11);
    else
      Move randomly using Eq.(12);
    end
    Check boundaries and evaluate $\overrightarrow{X_{i-BOA}}$;
    Update $\overrightarrow{X_i}$, $gbestvalue$ and $\overrightarrow{gbest}$, FEs;
  end
  for $i = 1$ ***to*** N **do**
    Calculate $\overrightarrow{X_{learning}}$ by Eq.(17);
    Update position using Eq.(18);
    Check boundaries and evaluate $\overrightarrow{X_{i-CL}}$;
    Update $\overrightarrow{X_i}$, $gbestvalue$ and $\overrightarrow{gbest}$, FEs;
  end
  Eliminate and initialize using Eq.(19);
end

TABLE I
ALGORITHM AND PARAMETERS SETTING.

Algorithm	Ref.	Year	Parameters setting
BOA	[22]	2019	p=0.8, c=0.01
GGWO	[28]	2022	A=2*a*rand-a, C=2*rand, σ=0.5
WPBOA	[26]	2021	p=0.8, c=0.01, w_{max}=0.8, w_{min}=0.2
EWOA	[29]	2022	C= 2*rand, b=1
GQPSO	[30]	2010	w_1=0.5, w_2=1.0, c_1=1.5, c_2=1.5
ESO	[27]	2023	r_1=rand, r_2=0.5, δ_{max}=10, δ_{min}=9
mSCBOA	[31]	2022	c=0.01, r_2=2*pi*rand, sa=2
MABOA	[32]	2021	p=0.8, a=0.1, c_0=0.01, N=220, λ=2
HHO	[33]	2019	E=2*(1-t/T)
CTBOA	Pres.	Pres.	p=0.8, c=0.01

TABLE II
THE FUNCTIONS INFORMATION OF CEC2022.

Type	No.	Function	f_{opt}
Unimodal	f_1	Shifted and full Rotated Zakharov	300
Basic	f_2	Shifted and full Rotated Rosenbrock's	400
	f_3	Shifted and full Rotated Expanded Schaffer's f_6	600
	f_4	Shifted and full Rotated Non-Continuous Rastrigin's	800
	f_5	Shifted and full Rotated Lévy	900
Hybrid	f_6	Hybrid 1 (N=3)	1800
	f_7	Hybrid Function 2 (N=6)	2000
	f_8	Hybrid Function 3 (N=5)	2200
Composition	f_9	Composition 1 (N=5)	2300
	f_{10}	Composition (N=4)	2400
	f_{11}	Composition (N=5)	2600
	f_{12}	Composition (N=6)	2700

* Search range: [-100,100], f_{opt}: The optimal solution.

C. Comparing CTBOA with 9 well-known algorithms

In this subsection, the proposed algorithm is contrasted with the methods in Table I, and the results for 10 dimensions is shown in Table II. The comparison is carried out with respect to mean (Mean), standard deviation (Std) and minimum (Best), worst (Worst), respectively. From it, the comprehensive performance of CTBOA is superior to that of other 9 advanced comparison algorithms. On D10, f_2, f_6, f_8, f_9, f_{10}, and f_{11} obtain optimal averages, but perform less well on some of the test functions, such as f_5 and f_7.

D. Population diversity analysis

From Table II, it is clear that f_2 perform excellent. In order to investigate the causes of CTBOA's excellent performance, the diversity is evaluated and the results are presented in Figure 6. The figure shows that, in the whole iteration process, despite different dimensions, CTBOA has better population diversity than BOA, which is favorable for searching high accuracy solutions.

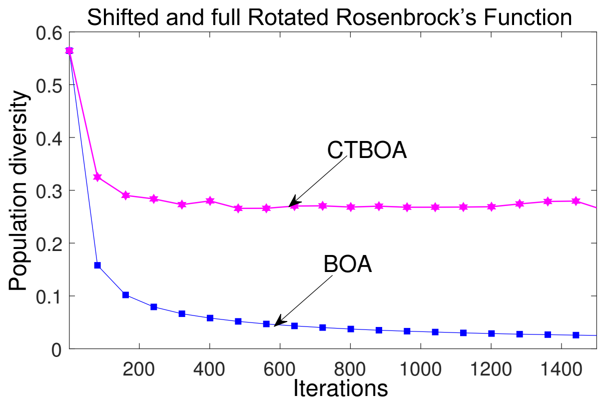

Fig. 6: Diversity analysis of BOA and CTBOA for f_2 on D10.

E. Convergence preference

For a more all-round assessment of the proposed algorithm's performance, in this section, basic function f_2 and hybrid function f_6 in CEC2022 test suite are employed to assess the convergence performance of CTBOA, and the results is illustrated in Figure 7. It is evident in Figure 7 that on 10 dimensions, CTBOA has satisfactory convergence speed and accuracy against the 9 compared algorithms. Collectively, CTBOA has excellent overall performance on basic function and hybrid function.

F. Non-parametric tests

In this subsection, three non-parametric statistics, Friedman [34], Friedman aligned rank [35] and Wilcoxon signed rank [36] are used to test if there is a significant difference between CTBOA and comparison methods, and the experimental results are shown in Tables III and IV.

1) Friedman rank and Friedman aligned rank test : The Friedman rank test is a powerful non-parametric testing method, and its core is a statistical means based on rank. This unique method skillfully reduces the potential impact of data distribution patterns on the results by performing

TABLE III
EXPERIMENTAL RESULTS OF CTBOA AND CONTRASTING METHODS ON D10.

Fun	Index	BOA	GGWO	WPBOA	EWOA	GQPSO	ESO	mSCBOA	MABOA	HHO	CTBOA
f_1	Mean	7.45381000E+03	3.28232200E+02	2.79386352E+03	3.00000000E+02	1.90918257E+03	3.00591921E+02	4.13606739E+03	8.52390510E+03	3.02280468E+02	3.00324396E+02
	Std	3.21778613E+03	8.39527152E+00	9.35886969E+02	2.55740931E-13	2.55697362E+02	6.45211328E-01	2.29571086E+03	4.67455792E+03	1.24146761E+00	1.21138497E-01
	Best	1.79583710E+03	3.14185220E+02	1.17564767E+03	3.00000000E+02	1.25040394E+03	3.00000662E+02	8.82214093E+02	1.13414438E+03	3.00418536E+02	3.00109605E+02
	Worst	1.53489468E+04	3.40566707E+02	4.48334432E+03	3.00000000E+02	2.29831316E+03	3.02373429E+02	9.73373844E+03	1.96597370E+04	3.06103162E+02	3.00546838E+02
	Rank	9	5	7	1	6	3	8	10	4	2
f_2	Mean	2.53851321E+03	4.08355346E+02	6.15760550E+02	4.08150025E+02	5.07501615E+02	4.13546365E+02	1.12450750E+03	9.28138258E+02	4.21035581E+02	4.00960893E+02
	Std	1.13249933E+03	2.68804163E+00	6.40216540E+01	1.24284849E+00	1.78180528E+01	2.45238480E+01	5.00707114E+02	3.83337241E+02	2.81863146E+01	1.77009748E+00
	Best	6.47352254E+02	4.02573147E+02	4.81177090E+02	4.04126327E+02	4.41422718E+02	4.00000542E+02	5.68927927E+02	4.62981599E+02	4.00033770E+02	4.00023128E+02
	Worst	4.58097410E+03	4.11856685E+02	7.53200944E+02	4.08916102E+02	5.31521154E+02	4.85968059E+02	2.90255219E+03	1.94359667E+03	4.76780657E+02	4.07277357E+02
	Rank	10	3	7	2	6	4	9	8	5	1
f_3	Mean	6.58085778E+02	6.04748720E+02	6.34680131E+02	6.02570106E+02	6.29366758E+02	6.03629895E+02	6.48509761E+02	6.41264236E+02	6.33499830E+02	6.14204619E+02
	Std	8.37438718E+00	1.18741380E+00	5.17231722E+00	3.88106234E+00	3.15814139E+00	2.61550608E+00	1.12979297E+01	1.06688214E+01	1.48906190E+01	4.95986640E+00
	Best	6.35207449E+02	6.03172718E+02	6.21708183E+02	6.00013124E+02	6.20085761E+02	6.00085108E+02	6.29572880E+02	6.21447382E+02	6.03794598E+02	6.05686922E+02
	Worst	6.69459776E+02	6.08389455E+02	6.41694319E+02	6.14907101E+02	6.33923490E+02	6.08889274E+02	6.72008703E+02	6.66982043E+02	6.60277739E+02	6.23491770E+02
	Rank	10	3	7	1	5	2	9	8	6	4
f_4	Mean	8.40865914E+02	8.18934681E+02	8.40584135E+02	8.29894744E+02	8.32570554E+02	8.13669338E+02	8.56111639E+02	8.52815085E+02	8.25278391E+02	8.14787558E+02
	Std	1.05651459E+01	3.60816038E+00	4.89816898E+00	1.03159579E+01	2.87574612E+00	5.97424708E+00	1.02322289E+01	1.07999942E+01	7.79762472E+00	3.56155968E+00
	Best	8.21819996E+02	8.09408383E+02	8.26330820E+02	8.10944545E+02	8.27463372E+02	8.04974795E+02	8.37363923E+02	8.26490769E+02	8.06060571E+02	8.04343063E+02
	Worst	8.65020194E+02	8.24318597E+02	8.47590277E+02	8.47271545E+02	8.37852273E+02	8.26984527E+02	8.72512711E+02	8.67617699E+02	8.43940644E+02	8.21496708E+02
	Rank	8	3	7	5	6	1	10	9	4	2
f_5	Mean	1.90515184E+03	9.03354795E+02	1.18439177E+03	9.36971555E+02	1.03372030E+03	9.01370316E+02	1.55461499E+03	1.22431295E+03	1.29748912E+03	9.85653733E+02
	Std	4.07373197E+02	8.67432888E-01	6.60227400E+01	3.70521655E+01	1.93295495E+01	3.52873684E+00	2.59139151E+02	2.00843063E+02	1.77582170E+02	3.54597848E+01
	Best	1.10836307E+03	9.02230381E+02	1.05820171E+03	9.00543852E+02	9.97110929E+02	9.00000256E+02	1.10659045E+03	9.10546636E+02	1.00856006E+03	9.20404817E+02
	Worst	2.61348317E+03	9.04959318E+02	1.31837908E+03	1.07179510E+03	1.08671580E+03	9.17333151E+02	2.04100212E+03	1.76727359E+03	1.63271727E+03	1.05046806E+03
	Rank	10	2	6	3	5	1	9	7	8	4
f_6	Mean	2.70966603E+07	1.23889551E+04	3.67938820E+06	4.62143895E+03	9.97022435E+05	2.92402661E+03	3.28129867E+06	5.15072773E+06	2.61477370E+03	2.04603987E+03
	Std	4.06182145E+07	7.56230540E+03	3.23930634E+06	2.16872117E+03	6.18906159E+05	1.27058468E+03	1.33796046E+07	1.64930298E+07	8.18334394E+02	9.69438987E+01
	Best	7.25924703E+04	2.24806085E+03	5.23834814E+05	1.82994311E+03	7.60371711E+04	1.83044478E+03	2.04411723E+03	4.74104660E+03	1.88063494E+03	1.92155777E+03
	Worst	3.63135153E+08	3.38932376E+04	1.51392929E+07	8.10245362E+03	2.55578334E+06	5.92664906E+03	7.28172099E+07	7.15819547E+07	5.57885590E+03	2.36186752E+03
	Rank	10	5	8	4	6	3	7	9	2	1
f_7	Mean	2.09868616E+03	2.02735854E+03	2.06732667E+03	2.02351035E+03	2.07132608E+03	2.02659536E+03	2.10841535E+03	2.08867137E+03	2.06853774E+03	2.03061856E+03
	Std	2.49256000E+01	3.68867567E+00	5.78761105E+00	6.60579638E+00	8.13337681E+00	1.92943084E+01	3.08117846E+01	2.35064669E+01	3.53581562E+01	6.24970463E+00
	Best	2.03521484E+03	2.01821942E+03	2.05253075E+03	2.00198992E+03	2.04990636E+03	2.00266198E+03	2.05692131E+03	2.04373172E+03	2.02829746E+03	2.02170300E+03
	Worst	2.13916241E+03	2.03285211E+03	2.08149928E+03	2.04128126E+03	2.08487021E+03	2.10412173E+03	2.16178578E+03	2.14648495E+03	2.15025311E+03	2.04046920E+03
	Rank	9	3	5	1	7	2	10	8	6	4
f_8	Mean	2.84187221E+03	2.21849233E+03	2.23513231E+03	2.22313096E+03	2.23036382E+03	2.21968435E+03	2.24287696E+03	2.26498518E+03	2.22926057E+03	2.21761828E+03
	Std	2.48059556E+03	6.51664624E+00	3.30026216E+00	3.00992379E+00	1.77051592E+00	5.20866561E+00	1.91740200E+01	5.24431961E+01	8.46110319E+00	6.99441181E+00
	Best	2.22977052E+03	2.20943795E+03	2.22725598E+03	2.21381980E+03	2.22633504E+03	2.20105888E+03	2.21718669E+03	2.22822263E+03	2.21680039E+03	2.20575370E+03
	Worst	1.08282255E+04	2.22642918E+03	2.24281684E+03	2.23006743E+03	2.23455709E+03	2.22582305E+03	2.27854686E+03	2.36409683E+03	2.25921918E+03	2.22760759E+03
	Rank	10	2	7	4	6	3	8	9	5	1
f_9	Mean	2.81214655E+03	2.53022001E+03	2.64007763E+03	2.53276634E+03	2.62666838E+03	2.53908733E+03	2.75410329E+03	2.73028497E+03	2.54418337E+03	2.52297019E+03
	Std	8.67186542E+01	2.88177664E-01	2.37694377E+01	7.56848380E+00	1.20142439E+01	3.72776431E+01	4.64332795E+01	4.56275134E+01	4.47697378E+01	3.75657839E+01
	Best	2.67339037E+03	2.52977320E+03	2.58137926E+03	2.52928438E+03	2.59678179E+03	2.52928438E+03	2.65737966E+03	2.66808474E+03	2.52930216E+03	2.32407912E+03
	Worst	3.06723125E+03	2.53082956E+03	2.67043853E+03	2.54940589E+03	2.65194250E+03	2.67622952E+03	2.84960158E+03	2.84778600E+03	2.67623929E+03	2.53083200E+03
	Rank	10	2	7	3	6	4	9	8	5	1
f_{10}	Mean	2.58933720E+03	2.50050897E+03	2.51664339E+03	2.50099431E+03	2.54176598E+03	2.56791303E+03	2.83267476E+03	2.76931330E+03	2.60455283E+03	2.50044949E+03
	Std	1.28264256E+02	9.22414770E-02	3.63257901E+00	3.09783352E-01	6.23936042E+01	6.73151481E+01	4.41122794E+02	3.97410653E+02	5.88624523E+01	9.76656547E-02
	Best	2.50076344E+03	2.50028941E+03	2.50701568E+03	2.50029556E+03	2.50198553E+03	2.42415900E+03	2.51186572E+03	2.50441690E+03	2.50053110E+03	2.50026116E+03
	Worst	3.32928053E+03	2.50075219E+03	2.52289162E+03	2.50156814E+03	2.65075155E+03	2.65317494E+03	4.20090939E+03	4.25606390E+03	2.65709215E+03	2.50061905E+03
	Rank	7	2	4	3	5	6	10	9	8	1
f_{11}	Mean	3.23183075E+03	2.65090006E+03	2.92814997E+03	2.72478092E+03	2.80310407E+03	2.75413355E+03	3.44823370E+03	3.39930901E+03	2.76304857E+03	2.60659199E+03
	Std	3.20120465E+02	7.07533798E+00	4.84717078E+01	7.03141212E+01	1.67837402E+01	1.41473155E+02	5.19712459E+02	4.62089978E+02	1.44036729E+02	2.76334050E+00
	Best	2.86361899E+03	2.62522181E+03	2.83977398E+03	2.60000000E+03	2.75852975E+03	2.60001698E+03	2.88313208E+03	2.81466291E+03	2.60281920E+03	2.60307705E+03
	Worst	4.39019107E+03	2.66392918E+03	3.04453744E+03	2.76826638E+03	2.83004917E+03	3.00001984E+03	4.75470414E+03	4.46782559E+03	3.00203574E+03	2.61519691E+03
	Rank	8	2	7	3	6	4	10	9	5	1
f_{12}	Mean	2.93415457E+03	2.86220438E+03	2.91154028E+03	2.86538830E+03	2.92037323E+03	2.87135962E+03	2.99821095E+03	2.98265283E+03	2.89647639E+03	2.86336064E+03
	Std	5.90861572E+01	1.20041229E+00	1.10097517E+01	2.18513775E+00	5.72574236E+00	1.14629981E+01	1.08607275E+02	7.90062464E+01	5.07673441E+01	1.52368798E+00
	Best	2.87462560E+03	2.85987287E+03	2.89397850E+03	2.85966084E+03	2.91161427E+03	2.86405089E+03	2.87486125E+03	2.87478096E+03	2.86544548E+03	2.85958889E+03
	Worst	3.05730402E+03	2.86444810E+03	2.93715835E+03	2.87006711E+03	2.93455739E+03	2.90573140E+03	3.27182200E+03	3.28626127E+03	3.11866365E+03	2.86681672E+03
	Rank	8	1	6	3	7	4	10	9	5	2
	Total rank	109	33	78	33	71	37	109	103	63	24
	Final rank	9	2	7	3	6	4	10	8	5	1

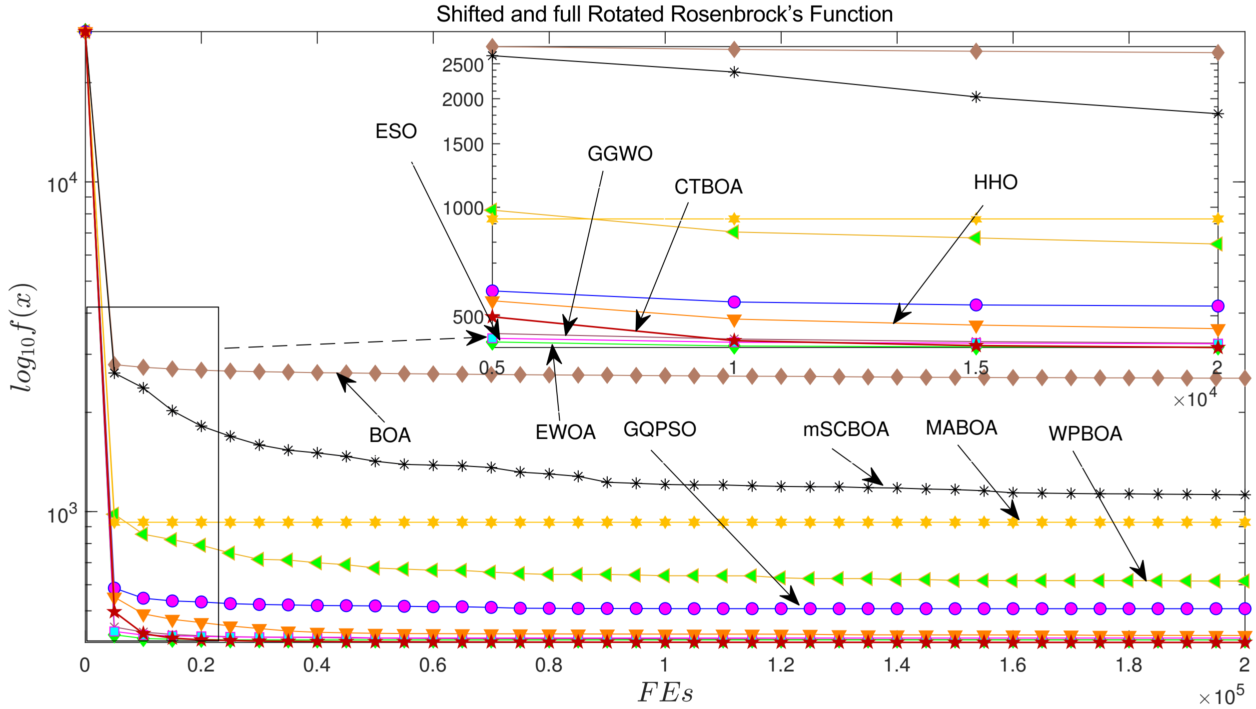

(a) f_2

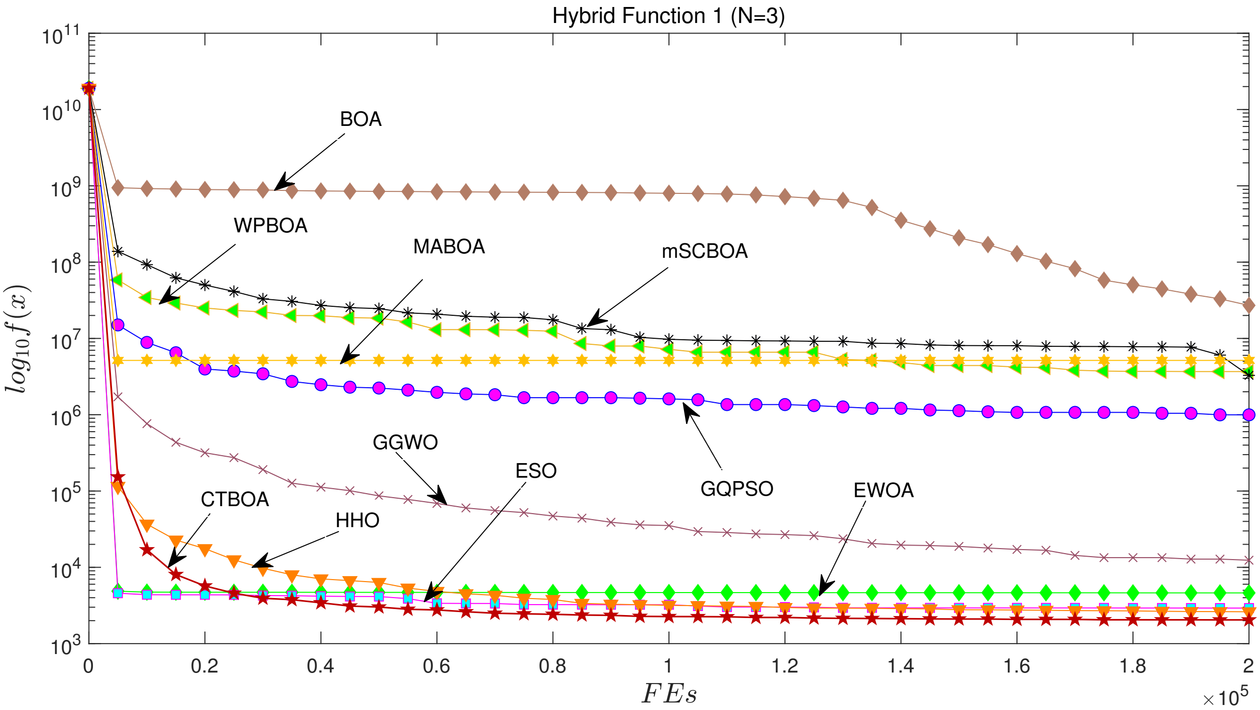

(b) f_6

Fig. 7: Convergence curves of CTBOA and the comparison methods on D10.

a sorting operation on the data. It is noteworthy that the significant advantage of the Friedman rank test lies in that it is completely independent of the data distribution form. This characteristic enables it to exhibit outstanding adaptability and reliability in the face of various complex data types and distribution situations, providing a more flexible and stable approach for statistical analysis. The bar chart shown in Figures 8 and 9 presents the results of the Friedman aligned rank test and the Friedman rank test of CTBOA and the comparative algorithms on D10 intuitively and clearly. The results show that CTBOA ranks the highest among all the tests and the p-values is much less than 0.05, it shows that there is a remarkable discrepancy between CTBOA and other methods.

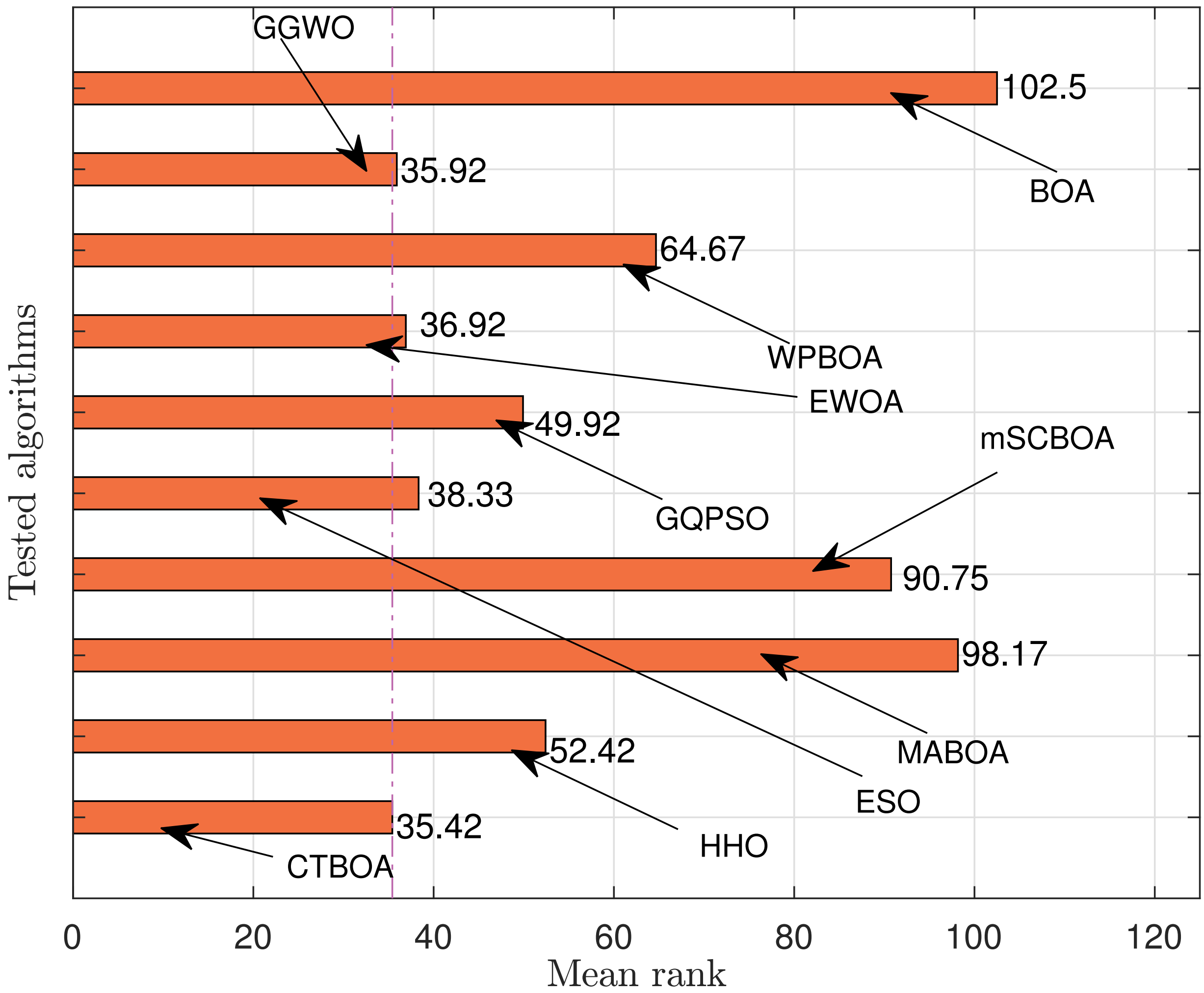

Fig. 8: Friedman alignment rank test results of CTBOA with compared algorithms.

2) Wilcoxon signed rank test: Wilcoxon signed rank test is a paired comparison method, it can be used to determine which algorithm has better statistical performance when comparing different benchmark functions. The outcomes of Wilcoxon signed rank test for the algorithm in Table I are shown in Table IV. 'R-' and 'R+' represent CTBOA better and worse than the contrasting methods, separately. '+/=/-' indicates a win, draw, and loss for CTBOA against the contrasting algorithm, correspondingly. From the Table IV, CTBOA holds a prominent edge over the comparison algorithms in relation to the majority of test functions.

TABLE IV
THE WILCOXON SIGNED-RANK (AVERAGE) RESULTS OF CTBOA AND CONTRASTING METHODS.

CTBOA vs.	p-Value	R_+	R_-	+/=/-
BOA	1.74994167E-06	0.08333333	464.91666667	12/0/0
GGWO	5.65471491E-02	170.00000000	295.00000000	7/2/3
WPBOA	1.73440000E-06	0.00000000	465.00000000	12/0/0
EWOA	1.17102237E-02	188.50000000	276.50000000	7/1/4
GQPSO	2.52861667E-06	1.58333333	463.41666667	12/0/0
ESO	3.61273750E-02	210.08333333	254.91666667	5/3/4
mSCBOA	1.78262500E-06	0.25000000	464.75000000	12/0/0
MABOA	2.06917500E-06	1.00000000	464.00000000	12/0/0
HHO	7.51303148E-03	42.08333333	422.91666667	11/1/0

G. Algorithm complexity analysis

To assess the complexity of the algorithm, in this part, I calculate the algorithm complexity on D10 for the proposed CTBOA and the comparison methods, and the corresponding outcomes are shown in Table V.

Where, the parameters in Table V are explained as follows. a) Run the test program '$x = 0.55; for\ i = 1 : 200000; x = x + x; x = x/2; x = x * x; x = sqrt(x); x = log(x); x = x/(x + 2); end$' and get the running time T_0, T_0 of this experiment platform is 0.003392; b) The computing time of 200000 FEs just for f_1 is T_1; c) The computing time for the random solutions with 200000 FEs of the same dimensional f_1 gives T_2; d) Perform step c) 5 times and get $\widehat{T_2}$=mean(T_2); e) The algorithm complexity is calculated by ($\widehat{T_2}$-T_1)/T_0.

As can be seen from the results in Table V, the algorithm complexity of CTBOA is 115.243943, which is only slightly higher than the original BOA, and has satisfactory algorithm complexity.

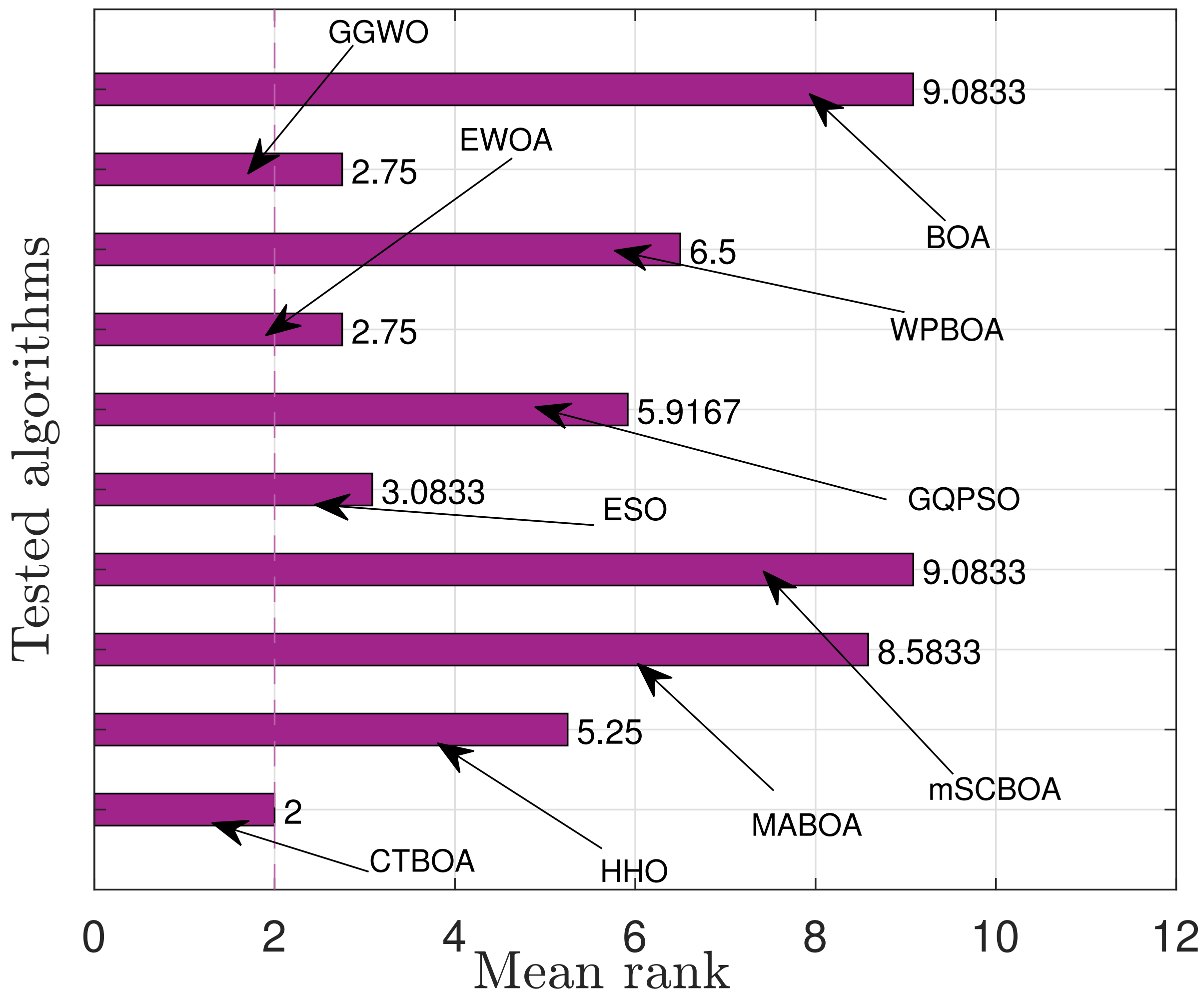

Fig. 9: Friedman rank test results of CTBOA with compared algorithms.

TABLE V
ALGORITHM COMPLEXITY OF CTBOA AND CONTRASTING ALGORITHMS ON D10.

Algorithm	T_0	T_1	$\widehat{T}_2$	$(\widehat{T}_2$-$T_1)/T_0$
BOA	0.00339170	0.92413660	1.30789602	113.14662853
HHO	0.00339170	0.89186150	1.22589752	98.48631070
MABOA	0.00339170	0.91764350	2.71866486	531.00845004
m_SCBOA	0.00339170	0.91221620	1.20306344	85.75264322
WPBOA	0.00339170	1.16332550	1.41652848	74.65370758
GGWO	0.00339170	1.03759620	2.21619894	347.49616417
GQPSO	0.00339170	1.03457850	1.53427294	147.32860807
EWOA	0.00339170	1.04033160	1.73994614	206.27253000
ESO	0.00339170	1.08083430	1.44341154	106.90132972
CTBOA	0.00339170	0.90149650	1.29236938	115.24394257

H. Runtime analysis

The runtime of an algorithm measures whether the algorithm can discover the optimal solution within a rational time frame. In the process of solving all test functions in the CEC2022 benchmark test set, the average running time of the proposed CTBOA and the comparison algorithm is depicted in Figure 10. As is evident from the figure, the running time of CTBOA is completely acceptable compared with other comparison methods.

V. APPLICATION RESULTS OF CTBOA TO PV MODELS

This section utilizes CTBOA to identify the parameters of the 4 PV models.

A. PV model parameter settings

The parameter information of the 3 experimented PV cell models (Case1-Case3) and 1 PV module model (Case4) are presented in this subsection, as presented in Table VI.The upper and lower bounds of the parameters to be identified in the four test cases are shown in Table VII.

B. Experimental results and analysis of PV cells

Within this subsection, CTBOA and contrast methods are utilized to identify the parameters of the 3 PV cells in Table VI. To conveniently observe the experimental results, a index of percentage improvement (IF) has been adopted, it is computed as per Eq.(20). IF is more than 0 indicating that CTBOA is better than the corresponding contrast method.

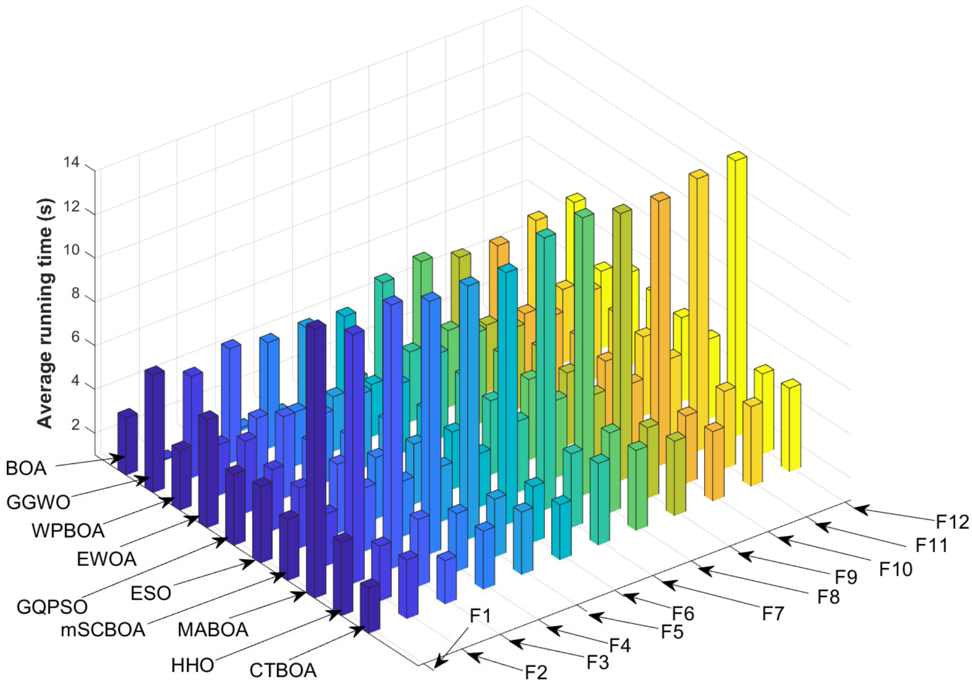

Fig. 10: Average running time of CTBOA and comparison methods on D10.

TABLE VI
PV MODELS INFORMATION.

Case	Type	Temperature	Irradiance	Modelling	Ref.
Case1	R.T.C France 57mm	33.00	1000	SDM	[37]
Case2	Amorphous Silicon	25.00	1000	DDM	[38]
Case3	Flexible Dual Junction	26.85	1000	TDM	[39]
Case4	Photowatt PWX500	25.00	1000	TDM	[40]

The maximum number of calculations for all experiments within this subsection, maximum number of calculations (maxFEs), is set to 100000 and the other parameters remain the same as those mentioned in Section IV. The parameter identification outcomes are given in Tables VII, VIII and IX, including the identification parameters corresponding to the optimal solution, the minimum RMSE, the running time, and the IF index.

$$IF = \frac{\min_{method} - \min_{CTBOA}}{\min_{method}} \cdot 100\% \tag{20}$$

From Table VII, CTBOA is capable of recognizing the 5 parameters of the R.T.C France 57mm PV cell model built in SDM with the highest accuracy and the shortest running time. Also, the IF index confirms that CTBOA has the smallest RMSE value. From Table VIII, the optimal RMSE value of Amorphous Silicon aSi:H, a PV cell model based on DDM identified by CTBOA, is 4.481564E-05, which is the minimum value among all algorithms, and the running time is slightly higher than the standard BOA, but still within the acceptable range. From Table IX, the 9 unknown parameters of the Flexible Dual Junction aSi with TDM identified by the proposed algorithm have the minimum RMSE, in other words, the highest parameter identification accuracy, and the running time is second only to the standard BOA, lower than other algorithms.

In summary, the proposed CTBOA has satisfactory performance in identifying unknown parameters of PV cells.

C. Experimental results and analysis of PV module model

For this subsection, CTBOA and contrusting methods are utilized to identify the PV module parameters determined by the TDM (Case4), and the optimal parameters identification results, corresponding RMSE values, IF indexes and running times are shown in Table XI. From this, the proposed CTBOA is capable of identifying the parameters of the PV module modeled with TDM with the highest accuracy and short runtime.

D. Average performance analysis

Within this subsection, the average performance of CTBOA is analyzed using the mean (Mean), standard deviation (Std), optimum (Best),worst (Worst) and average ranking (Rank) of the 4 PV model parameters identified in 30 runs, the consequences are presented at Table XII. It is obvious, CTBOA ranks first in the average RMSE value of the identification parameters on PV models, and finally ranks first in all test cases.

E. statistical analysis

Boxchart serve to show how discrete the data is. Figure 11 is the boxchart of the average RMSE obtained by the algorithms in Table I through 30 tests on 4 PV test cases. The '+' represents outliers, the width of the box reflects the extent of data fluctuation, and the central horizontal line indicates the median of the data. It is observable from the boxchart that CTBOA demonstrates remarkable accuracy in most test cases and exhibits a relatively stable performance.

TABLE VII
THE INFORMATION AND LIMITS OF PV MODELS.

Case	Material	Dimension	I_{ph} (A)	I_{sd1} (A)	I_{sd2} (A)	I_{sd3} (A)	R_s (Ω)	R_p (Ω)	n_1	n_1	n_1
Case1	Silicon	5	[0,1]	[1e-12,1e-6]	/	/	[0.001,0.5]	[0.001,100]	[1,2]	/	/
Case2	Amorphous Silicon	7	[0,1]	[1e-12,1e-6]	[1e-12,1e-6]	/	[0.001,0.5]	[0.001,100]	[1,5]	[1,5]	/
Case3	Amorphous Silicon	9	[0,1]	[1e-15,1e-6]	[1e-15,1e-6]	[1e-15,1e-6]	[0.001,0.5]	[0.001,100]	[1,2]	[1,2]	[1,2]
Case4	Polycrystalline	9	[0,3.5]	[1e-12,5e-5]	[1e-12,5e-5]	[1e-12,5e-5]	[0.001,0.5]	[0.001,1000]	[1,2]	[1,2]	[1,2]

TABLE VIII
RESULTS OF PARAMETER IDENTIFICATION OF CTBOA AND COMPARISON METHODS FOR CASE1.

Method	I_{ph} (A)	I_{sd1} (A)	R_s (Ω)	R_p (Ω)	n_1	RMSE	IF (%)	Time (s)
BOA	0.76222533	5.04953506E-07	0.03567444	68.21693417	1.52708912	2.51209681E-03	6.07490311E-01	2.72936130
GGWO	0.76067424	3.54008365E-07	0.03608943	59.83301632	1.49036350	1.02254763E-03	3.57198892E-02	4.30606570
WPBOA	0.76268538	9.43619873E-07	0.02830388	46.02972964	1.60022257	7.46748448E-03	8.67957899E-01	3.32919870
EWOA	0.76072997	3.32476626E-07	0.03630350	55.59820737	1.48405412	9.91111232E-04	5.13453347E-03	4.65686450
GQPSO	0.77390438	3.77238175E-07	0.03585747	20.56862571	1.49922633	8.91047885E-03	8.89341263E-01	5.03563260
ESO	0.76005452	9.99885109E-07	0.03113397	89.89996458	1.60484162	2.60717506E-03	6.21804322E-01	3.16263220
mSCBOA	0.78098269	7.85332054E-07	0.03410737	39.32611331	1.57070234	1.80152175E-02	9.45267253E-01	3.31036220
MABOA	0.77768499	4.86895057E-07	0.03849074	53.67321001	1.52330459	1.46420931E-02	9.32658375E-01	7.67321250
HHO	0.76167978	5.44760047E-07	0.03373696	52.13084769	1.53605123	1.69488206E-03	4.18235426E-01	3.88796190
CTBOA	0.76074566	3.33891498E-07	0.03624417	54.89722022	1.48451911	9.86022338E-04	0	2.54412220

TABLE IX
RESULTS OF PARAMETER IDENTIFICATION OF CTBOA AND COMPARISON METHODS FOR CASE2.

Method	I_{ph} (A)	I_{sd1} (A)	I_{sd2} (A)	R_s (Ω)	R_p (Ω)	n_1	n_2	RMSE	IF (%)	Time (s)
BOA	0.01128024	2.55277893E-07	2.61741377E-07	0.27629536	571.45039349	3.22063018	3.26568830	6.77319056E-05	3.38337810E-01	2.37196030
GGWO	0.01135354	4.10998439E-07	3.87099951E-07	0.27378390	515.87726140	3.20585939	4.10616503	4.64562897E-05	3.53159657E-02	4.68668090
WPBOA	0.01145473	9.95691097E-07	2.07696731E-07	0.09305533	427.78206045	4.77681263	3.00449092	7.97073524E-05	4.37747716E-01	3.48311010
EWOA	0.01135615	1.00000000E-06	2.96920032E-08	0.50000000	524.98335609	3.69789773	2.70346956	4.49003358E-05	1.88628605E-03	4.47135580
GQPSO	0.01141012	3.50496844E-07	2.92714146E-07	0.20480178	419.24935945	3.18782850	3.74889388	1.17684471E-04	6.19188152E-01	3.69727650
ESO	0.01134233	5.49446685E-08	1.00000000E-06	0.20307256	531.95728960	2.85368818	3.69450427	4.51832168E-05	8.13523012E-03	3.58244990
mSCBOA	0.01126181	7.42047547E-07	7.42047547E-07	0.37076739	742.04754673	3.62108008	3.62108008	1.03918893E-04	5.68744051E-01	4.09462650
MABOA	0.01167576	4.50835181E-07	5.85178647E-07	0.27193681	400.02347324	3.44657126	4.22149177	8.66303422E-04	9.48267963E-01	7.70649750
HHO	0.01133591	2.80242408E-07	1.84551498E-07	0.46246683	511.71656231	3.08780026	3.73116616	5.80984226E-05	2.28625512E-01	3.77745900
CTBOA	0.01135510	1.04758715E-08	1.00000000E-06	0.50000000	527.02846195	2.53979120	3.62991062	4.48156409E-05	0	3.76499100

TABLE X
RESULTS OF PARAMETER IDENTIFICATION OF CTBOA AND COMPARISON METHODS FOR CASE3.

Method	I_{ph} (A)	I_{sd1} (A)	I_{sd2} (A)	I_{sd3} (A)	R_s (Ω)	R_p (Ω)	n_1	n_2	n_3	RMSE	IF (%)	Time (s)
BOA	0.36298922	1.00000000E-15	1.00000000E-15	1.00000000E-15	0.02462644	64.94758749	1.48353350	1.49663708	1.50676359	1.98154423E+02	9.99922267E-01	2.37761660
GGWO	0.31938489	2.27819021E-14	6.74627016E-15	4.09824046E-15	0.42577491	14.71709070	1.99979848	1.99999998	1.99999991	1.54163179E-02	8.49009969E-04	4.23999240
WPBOA	0.21719273	1.00000000E-15	1.00000000E-15	1.00000000E-15	0.50000000	100.00000000	1.86351459	1.86351459	1.86351459	3.49867403E-02	5.59740943E-01	3.27955620
EWOA	0.32114700	1.00000000E-15	1.00000000E-15	1.00000000E-15	0.43874425	13.90599627	1.84979128	1.84979037	1.84978966	1.62321450E-02	5.10663061E-02	3.40365590
GQPSO	0.17461085	1.00000000E-15	1.00000000E-15	1.00000000E-15	0.05814366	59.28619631	1.80229632	1.95964592	2.00000000	4.85983435E-02	6.83050323E-01	3.94746620
ESO	0.31973805	2.67072457E-14	5.73931239E-15	1.03136191E-15	0.42276335	14.55389240	2.00000000	2.00000000	2.00000000	1.54032293E-02	1.65552525E-14	3.74726920
mSCBOA	0.51746707	7.39856563E-15	7.39856563E-15	7.39856563E-15	0.25562361	4.01888196	2.00000000	2.00000000	2.00000000	5.08006552E-02	6.96790735E-01	3.32514810
MABOA	0.25417640	1.10305259E-15	1.10305259E-15	1.10305259E-15	0.14716962	7.17849467	2.00000000	2.00000000	2.00000000	7.24153783E-02	7.87293394E-01	7.55774580
HHO	0.28818285	1.12043971E-15	1.12043971E-15	1.12047058E-15	0.46938956	26.77458280	1.85146794	1.85123709	1.85143844	1.82476898E-02	1.55880580E-01	3.28662260

TABLE XI
RESULTS OF PARAMETER IDENTIFICATION OF CTBOA AND COMPARISON METHODS FOR CASE4.

Method	I_{ph} (A)	I_{sd1} (A)	I_{sd2} (A)	I_{sd3} (A)	R_s (Ω)	R_p (Ω)	n_1	n_2	n_3	RMSE	IF (%)	Time (s)
BOA	2.23708590	5.60532154E-11	2.24565227E-10	1.00000000E-12	0.00694344	583.47512485	1.38784481	1.00000000	1.00000000	8.27449556E-01	9.83878817E-01	3.55739150
GGWO	3.20202408	1.70760001E-06	2.26208329E-06	4.17790350E-06	0.00309924	6.00769790	1.81436272	1.99357088	1.77641161	1.37681828E-02	3.11382224E-02	4.55318670
WPBOA	3.42916258	1.00000000E-12	2.88023975E-05	1.00000000E-12	0.00100000	1000.00000000	1.34510402	2.00000000	2.00000000	2.23320843E-01	9.40267707E-01	3.21789080
EWOA	3.21375794	3.78969483E-06	1.00000000E-12	1.00000000E-12	0.00394158	4.51104274	1.71800911	1.00000000	1.00000000	1.38488023E-02	3.67783598E-02	3.65322920
GQPSO	3.20473262	1.00000000E-12	1.00000000E-12	1.99376017E-10	0.01145236	2.14316227	1.00000000	1.00000000	1.00000000	6.89186963E-02	8.06446338E-01	3.67524750
ESO	3.20808606	5.75938237E-06	2.28228103E-06	1.00000000E-12	0.00298509	5.42829556	1.78276168	2.00000000	2.00000000	1.33430020E-02	2.65006210E-04	3.20870900
mSCBOA	3.15743273	2.41417680E-06	7.83790310E-07	9.52118655E-08	0.00829117	190.46295393	1.69824931	1.69824931	1.69824931	7.59706592E-02	8.24412922E-01	3.63372740
MABOA	3.50000000	4.70674072E-06	1.85328638E-06	2.81771935E-05	0.01094833	3.80363719	2.00000000	2.00000000	2.00000000	5.28194741E-01	9.74745174E-01	8.10735560
HHO	3.18369295	1.00195457E-12	1.00184386E-12	2.58824677E-05	0.00102578	19.20216801	1.90190459	1.99438894	1.99441764	1.74642468E-02	2.36184291E-01	3.41241020
CTBOA	3.20982132	1.42017955E-11	2.01307501E-06	5.10180342E-06	0.00316619	5.15449210	1.50733131	1.99947162	1.76518093	1.33394661E-02	0	3.35744390

TABLE XII
PERFORMANCE (AVERAGE) FOR PARAMETER IDENTIFICATION OF CTBOA AND COMPARISON METHODS ON 4 PV MODELS.

Case	Index	BOA	GGWO	WPBOA	EWOA	GQPSO	ESO	mSCBOA	MABOA	HHO	CTBOA
Case1	Mean	5.65048038E-02	1.81252543E-03	2.20188355E-02	1.12242396E-02	4.29637797E-02	3.56916665E-03	8.36704506E-02	9.27560943E-02	5.47467096E-03	1.09930417E-02
	Std	5.59204292E-02	3.74846828E-04	7.55897568E-03	1.59053934E-02	1.68561155E-02	8.35863242E-04	8.44713808E-02	7.00015014E-02	5.18785404E-03	1.60440083E-02
	Best	2.51209681E-03	1.02254763E-03	7.46748448E-03	9.86137904E-04	8.91047885E-03	2.50260029E-03	1.80152175E-02	1.46420931E-02	1.69488206E-03	9.88207738E-04
	Worst	2.52928515E-01	2.40084191E-03	3.38498309E-02	3.71424719E-02	8.03843273E-02	5.81997726E-03	2.90419551E-01	2.48564320E-01	2.35999099E-02	3.71424719E-02
	Rank	5	3	7	2	8	6	10	9	4	1
Case2	Mean	1.92344464E-03	4.92547671E-05	1.96638280E-04	6.69646140E-05	2.22825020E-04	8.55096893E-05	8.34961409E-04	2.36361899E-03	3.53863189E-04	4.98324649E-05
	Std	2.17872957E-03	1.67600982E-06	7.97267685E-05	9.45454515E-05	5.39908454E-05	7.50733499E-05	1.41758459E-03	1.68393339E-03	2.78287427E-04	1.60755930E-05
	Best	6.77319056E-05	4.64562897E-05	7.97073524E-05	4.48426596E-05	1.17684471E-04	4.48524021E-05	1.03918893E-04	8.66303422E-04	5.80984226E-05	4.48156409E-05
	Worst	7.40516740E-03	5.41328311E-05	4.01492920E-04	5.63465667E-04	3.31497718E-04	4.34646212E-04	7.67570251E-03	8.67196649E-03	8.82294314E-04	1.33435761E-04
	Rank	6	4	7	2	9	3	8	10	5	1
Case3	Mean	5.69393258E+06	1.60484426E-02	4.65010019E+01	4.64113687E-02	2.05748590E+06	1.84224593E-02	5.78068712E+00	9.30258526E+05	2.53803382E-02	1.93675271E-02
	Std	3.78995542E+06	2.17758701E-03	2.53911443E+02	5.24390225E-02	7.37442477E+06	3.58042103E-03	6.33933735E+00	8.64577958E+05	6.03220269E-03	3.69783152E-03
	Best	1.98154423E+02	1.54163179E-02	3.49867403E-02	1.54032293E-02	4.85983435E-02	1.54032498E-02	5.08006552E-02	7.24153783E-02	1.82476898E-02	1.54032293E-02
	Worst	1.22473853E+07	2.46390303E-02	1.39087357E+03	1.48929810E-01	3.74813921E+07	2.95267179E-02	1.75011745E+01	2.80946826E+06	4.26725341E-02	3.17425063E-02
	Rank	10	3	6	4	7	2	8	9	5	1
Case4	Mean	2.39543000E+00	1.91563614E-02	5.77534659E-01	1.72361293E-02	3.84990144E-01	1.85029417E-02	2.03351445E+00	6.37815697E+00	2.91131688E-02	1.70203922E-02
	Std	4.52478425E-01	1.83603874E-03	2.64057440E-01	2.25351959E-03	2.91322346E-01	4.91562203E-03	9.61903947E-01	9.10457270E+00	1.09404677E-02	3.01617857E-03
	Best	8.27449556E-01	1.37681828E-02	2.23320843E-01	1.55648603E-02	6.89186963E-02	1.33311247E-02	7.59706592E-02	5.28194741E-01	1.74642468E-02	1.33394661E-02
	Worst	2.69585119E+00	2.19754695E-02	1.03185117E+00	2.15449450E-02	7.32225506E-01	3.92746495E-02	2.90252416E+00	4.61405099E+01	5.27337839E-02	2.29330673E-02
	Rank	10	3	8	4	6	2	7	9	5	1
	Total rank	31	13	28	12	30	13	33	37	19	4
	Final rank	9	4	6	2	7	3	8	10	5	1

VI. CONCLUSION

To identify the parameters of PV cell and module models, a butterfly optimization algorithm with improved fragrance factor, chaotic learning strategy and final elimination strategy is proposed in this paper. Firstly, a novel fragrance factor is used to increase the speed of convergence. Secondly, a chaotic learning strategy is utilized to improve the convergence accuracy of the problem. Finally a final elimination strategy is used to improve the diversity of the population.

Statistical results from CEC2022 benchmark test set validate the superiority of CTBOA over 9 comparison methods. Then, CTBOA is applied to identify the parameters of 3 PV cells and 1 module model, the results show that the proposed method has satisfactory parameter identification accuracy and runtime. However, CTBOA in this paper is only used to solve single-objective optimization problems, and its optimization ability for multi-objective problems is unknown. As future work, I will consider further optimizing the algorithm and applying it to multi-objective optimization problems.

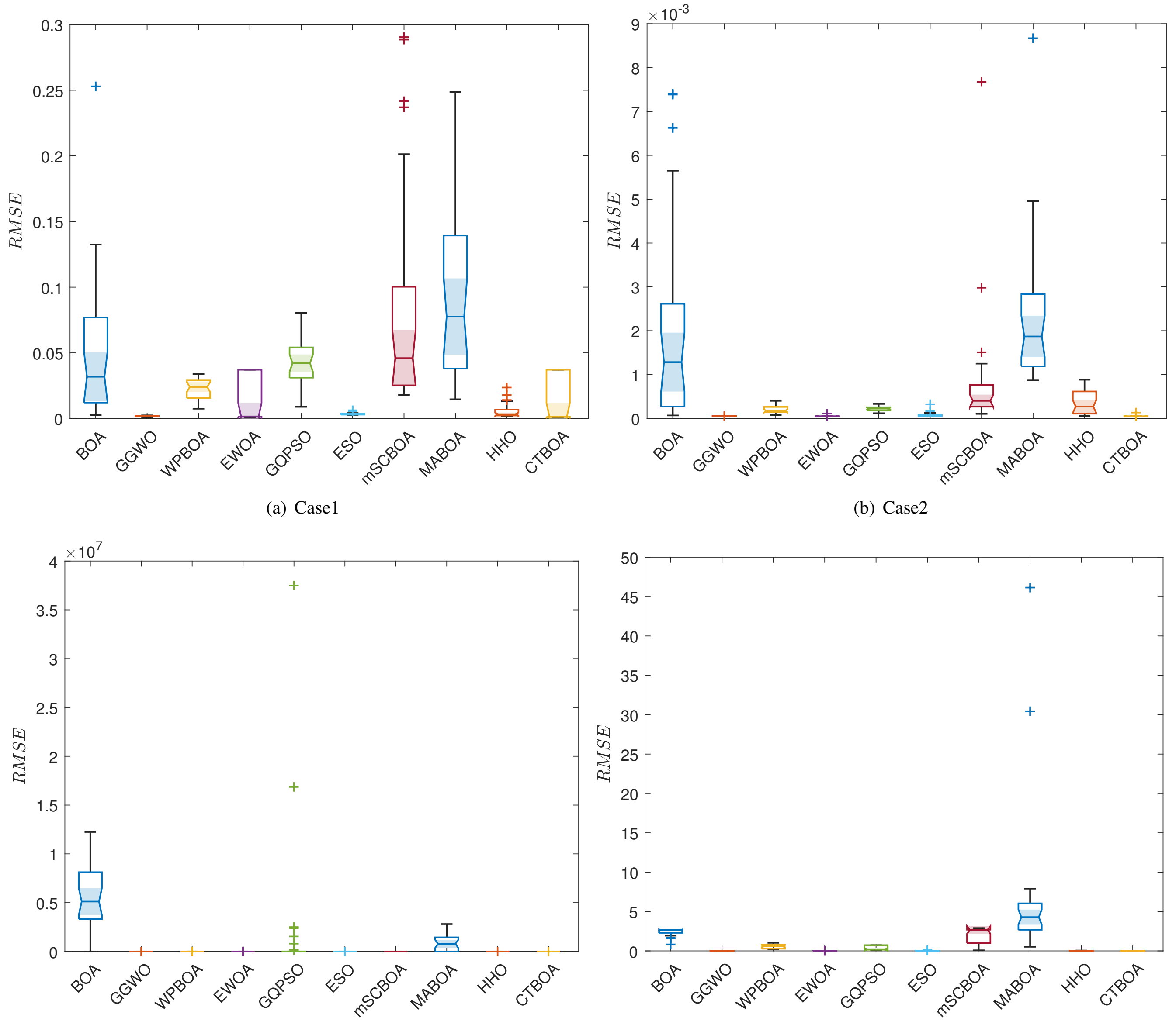

(a) Case1

(b) Case2

(c) Case3

(d) Case4

Fig. 11: Boxcharts of 4 PV models cases.

References

[1] M. Mao, L. Zhou, Z. Yang, Q. Zhang, C. Zheng, B. Xie, and Y. Wan, "A hybrid intelligent GMPPT algorithm for partial shading PV system," *Control Engineering Practice*, vol. 83, pp. 108–115, 2019.

[2] M. H. Qais, H. M. Hasanien, S. Alghuwainem, and A. S. Nouh, "Coyote optimization algorithm for parameters extraction of three-diode photovoltaic models of photovoltaic modules," *Energy*, vol. 187, p. 116001, 2019.

[3] R. Abbassi, A. Abbassi, A. A. Heidari, and S. Mirjalili, "An efficient salp swarm-inspired algorithm for parameters identification of photovoltaic cell models," *Energy Conversion and Management*, vol. 179, pp. 362–372, 2019.

[4] X. Gao, Y. Cui, J. Hu, G. Xu, Z. Wang, J. Qu, and H. Wang, "Parameter extraction of solar cell models using improved shuffled complex evolution algorithm," *Energy Conversion and Management*, vol. 157, pp. 460–479, 2018.

[5] J. Appelbaum and A. Peled, "Parameters extraction of solar cells - A comparative examination of three methods," *Solar Energy Materials and Solar Cells*, vol. 122, pp. 164–173, 2014.

[6] T. Wei, F. Yu, G. Huang, and C. Xu, "A Particle-Swarm-Optimization-Based Parameter Extraction Routine for Three-diode Lumped Parameter Model of Organic Solar Cells," *IEEE Electron Device Letters*, vol. 40, no. 9, pp. 1511–1514, 2019.

[7] Z. Xu and X. Zhang, "An Improve Grey Wolf Optimizer Algorithm for Traveling Salesman Problems," *IAENG International Journal of Computer Science*, vol. 51, no. 6, pp. 602–612, 2024.

[8] P. D. Kusuma, "Triple Shake Algorithm: A New Metaheuristic with Strict and Cross Dimension Mappings," *Engineering Letters*, vol. 32, no. 5, pp. 930–938, 2024.

[9] G. Xie, M. Zhang, M. Yang, and D. Wang, "Economic Dispatch of Isolated Microgrids Based on Enhanced Sparrow Search Algorithm," *Engineering Letters*, vol. 32, no. 4, pp. 753–760, 2024.

[10] J. Wang and Y. Wang, "An Efficient Improved Whale Optimization Algorithm for Optimization Tasks," *Engineering Letters*, vol. 32, no. 2, pp. 392–411, 2024.

[11] Y. Hou, C. Wang, W. Dong, and L. Dang, "An Improved Particle Swarm Optimization Algorithm for the Distribution of Fresh Products," *Engineering Letters*, vol. 31, no. 2, pp. 494–503, 2023.

[12] M. H. Qais and S. Muyeen, "A Novel Adaptive Filtering Algorithm Based Parameter Estimation Technique for Photovoltaic System," *IEEE Transactions on Energy Conversion*, vol. 37, no. 1, pp. 286–294, 2021.

[13] W. Zhou, P. Wang, A. A. Heidari, X. Zhao, H. Turabieh, and H. Chen, "Random learning gradient based optimization for efficient design of photovoltaic models," *Energy Conversion and Management*, vol. 230, p. 113751, 2021.

[14] B. Subudhi and R. Pradhan, "Bacterial Foraging Optimization Approach to Parameter Extraction of a Photovoltaic Module," *IEEE Transactions on Sustainable Energy*, vol. 9, no. 1, pp. 381–389, 2017.

[15] P. A. Kumari and P. Geethanjali, "Adaptive Genetic Algorithm Based Multi-Objective Optimization for Photovoltaic Cell Design Parameter Extraction," *Energy Procedia*, vol. 117, pp. 432–441, 2017.

[16] K. Yu, J. Liang, B. Qu, Z. Cheng, and H. Wang, "Multiple learning backtracking search algorithm for estimating parameters of photovoltaic models," *Applied Energy*, vol. 226, pp. 408–422, 2018.

[17] S. Li, Q. Gu, W. Gong, and B. Ning, "An enhanced adaptive differential evolution algorithm for parameter extraction of photovoltaic models," *Energy Conversion and Management*, vol. 205, p. 112443, 2020.

[18] H. Chen, S. Jiao, M. Wang, A. A. Heidari, and X. Zhao, "Parameters identification of photovoltaic cells and modules using diversification-enriched Harris hawks optimization with chaotic drifts," *Journal of Cleaner Production*, vol. 244, p. 118778, 2020.

[19] L. Peng, C. He, A. A. Heidari, Q. Zhang, H. Chen, G. Liang, N. O. Aljehane, and R. F. Mansour, "Information sharing search boosted whale optimizer with Nelder-Mead simplex for parameter estimation of photovoltaic models," *Energy Conversion and Management*, vol. 270, p. 116246, 2022.

[20] W. Long, J. Jiao, X. Liang, M. Xu, M. Tang, and S. Cai, "Parameters estimation of photovoltaic models using a novel hybrid seagull optimization algorithm," *Energy*, vol. 249, p. 123760, 2022.

[21] X. Yu, Y. Duan, and Z. Cai, "Sub-population improved grey wolf optimizer with Gaussian mutation and Lévy flight for parameters identification of photovoltaic models," *Expert Systems with Applications*, vol. 232, p. 120827, 2023.

[22] S. Arora and S. Singh, "Butterfly optimization algorithm: a novel approach for global optimization," *Soft Computing*, vol. 23, pp. 715–734, 2019.

[23] Y. Fan, J. Shao, G. Sun, and X. Shao, "A Self-Adaption Butterfly Optimization Algorithm for Numerical Optimization Problems," *IEEE Access*, vol. 8, pp. 88 026–88 041, 2020.

[24] D. Ustun, "An enhanced adaptive butterfly optimization algorithm rigorously verified on engineering problems and implemented to ISAR image motion compensation," *Engineering Computations*, vol. 37, no. 9, pp. 3543–3566, 2020.

[25] X. Chen, K. Yu, W. Du, W. Zhao, and G. Liu, "Parameters identification of solar cell models using generalized oppositional teaching learning based optimization," *Energy*, vol. 99, pp. 170–180, 2016.

[26] Y. Guo, X. Liu, and L. Chen, "Improved butterfly optimisation algorithm based on guiding weight and population restart," *Journal of Experimental & Theoretical Artificial Intelligence*, vol. 33, no. 1, pp. 127–145, 2021.

[27] L. Yao, P. Yuan, C.-Y. Tsai, T. Zhang, Y. Lu, and S. Ding, "ESO: An enhanced snake optimizer for real-world engineering problems," *Expert Systems with Applications*, vol. 230, p. 120594, 2023.

[28] M. H. Nadimi-Shahraki, S. Taghian, S. Mirjalili, H. Zamani, and A. Bahreininejad, "GGWO: Gaze cues learning-based grey wolf optimizer and its applications for solving engineering problems," *Journal of Computational Science*, vol. 61, p. 101636, 2022.

[29] M. H. Nadimi-Shahraki, H. Zamani, and S. Mirjalili, "Enhanced whale optimization algorithm for medical feature selection: A COVID-19 case study," *Computers in Biology and Medicine*, vol. 148, p. 105858, 2022.

[30] L. dos Santos Coelho, "Gaussian quantum-behaved particle swarm optimization approaches for constrained engineering design problems," *Expert Systems with Applications*, vol. 37, no. 2, pp. 1676–1683, 2010.

[31] S. Sharma, A. K. Saha, S. Roy, S. Mirjalili, and S. Nama, "A mixed sine cosine butterfly optimization algorithm for global optimization and its application," *Cluster Computing*, vol. 25, no. 6, pp. 4573–4600, 2022.

[32] K. Hu, H. Jiang, C.-G. Ji, and Z. Pan, "A modified butterfly optimization algorithm: An adaptive algorithm for global optimization and the support vector machine," *Expert Systems*, vol. 38, no. 3, p. e12642, 2021.

[33] A. A. Heidari, S. Mirjalili, H. Faris, I. Aljarah, M. Mafarja, and H. Chen, "Harris hawks optimization: Algorithm and applications," *Future Generation Computer Systems*, vol. 97, pp. 849–872, 2019.

[34] M. Friedman, "The Use of Ranks to Avoid the Assumption of Normality Implicit in the Analysis of Variance," *Journal of the American Statistical Association*, vol. 32, no. 200, pp. 675–701, 1937.

[35] S. García, A. Fernández, J. Luengo, and F. Herrera, "Advanced non-parametric tests for multiple comparisons in the design of experiments in computational intelligence and data mining: Experimental analysis of power," *Information Sciences*, vol. 180, no. 10, pp. 2044–2064, 2010.

[36] D. W. Zimmerman and B. D. Zumbo, "Relative Power of the Wilcoxon Test, the Friedman Test, and Repeated-Measures ANOVA on Ranks," *The Journal of Experimental Educational*, vol. 62, no. 1, pp. 75–86, 1993.

[37] X. Yu, Z. Hu, X. Wang, and W. Luo, "Ranking teaching–learning-based optimization algorithm to estimate the parameters of solar models," *Engineering Applications of Artificial Intelligence*, vol. 123, p. 106225, 2023.

[38] D. T. Cotfas, A. M. Deaconu, and P. A. Cotfas, "Hybrid successive discretisation algorithm used to calculate parameters of the photovoltaic cells and panels for existing datasets," *IET Renewable Power Generation*, vol. 15, no. 15, pp. 3661–3687, 2021.

[39] M. Louzazni and S. Al-Dahidi, "Approximation of photovoltaic characteristics curves using Bézier Curve," *Renewable Energy*, vol. 174, pp. 715–732, 2021.

[40] M. A. El-Dabah, R. A. El-Sehiemy, M. Becherif, and M. Ebrahim, "Parameter estimation of triple diode photovoltaic model using an artificial ecosystem-based optimizer," *International Transactions on Electrical Energy Systems*, vol. 31, no. 11, p. e13043, 2021.